NACA TN 2143

NATIONAL ADVISORY COMMITTEE FOR AERONAUTICS

TECHNICAL NOTE 2143

ANALYSIS OF THE EFFECTS OF BOUNDARY-LAYER CONTROL ON THE POWER-OFF LANDING PERFORMANCE CHARACTERISTICS OF A LIAISON TYPE OF AIRPLANE

By Elmer A. Horton, Laurence K. Loftin, Jr.,
and Stanley F. Racisz

Langley Aeronautical Laboratory
Langley Air Force Base, Va.

NACA

Washington

August 1950

NATIONAL ADVISORY COMMITTEE FOR AERONAUTICS

TECHNICAL NOTE 2143

ANALYSIS OF THE EFFECTS OF BOUNDARY-LAYER CONTROL ON THE POWER-OFF LANDING PERFORMANCE CHARACTERISTICS OF A LIAISON TYPE OF AIRPLANE

By Elmer A. Horton, Laurence K. Loftin, Jr., and Stanley F. Racisz

SUMMARY

A performance analysis has been made to determine whether boundary-layer control by suction might be effective in making the power-off landing distance of a liaison type of airplane less than that obtainable with conventional high-lift devices. The airplane was assumed to be operating from airstrips which would give a combined ground and braking friction coefficient of 0.4. The pay load was fixed at 1500 pounds, the wing span was varied from 25 to 100 feet, the aspect ratio was varied from 5 to 15, and the engine brake horsepower was varied from 300 to 1200. Maximum lift coefficients of 5.0 and 2.8 were assumed for the airplanes with and without boundary-layer control, respectively. A conservative estimate of the added weight due to the boundary-layer control equipment was included. The effects of boundary-layer control on the total landing distance, ground run, stalling speed, and sinking speed were investigated.

The results of the analysis indicate that for a specified airplane maximum speed, the total landing distance can be reduced from 25 to 40 percent by the use of boundary-layer control. A comparison of the results presented with those of a previous analysis of the effect of boundary-layer control on the take-off distance shows that boundary-layer control is much more effective in reducing the landing distance than the take-off distance. Boundary-layer control also reduced the ground-run distance, the stalling speed, and the gliding speed. The sinking speed, or vertical velocity, of the airplane with boundary-layer control was slightly higher than that for the conventional airplane having the same wing span.

INTRODUCTION

The design of a new airplane usually involves a compromise between several desired high-speed performance characteristics and the practical necessity for operating the airplane out of airports of reasonable size. The degree of necessary compromise has been reduced by the use of high-lift devices to increase the maximum lift coefficient. Such devices as leading- and trailing-edge flaps which are now in use on operational aircraft permit the attainment of maximum airplane lift coefficients, power-off, of the order of 2.80 (reference 1). In the belief that much higher airplane maximum lift coefficients would be desirable, numerous wind-tunnel investigations have been made of the effectiveness of boundary-layer control as a means for obtaining high maximum lift coefficients. Airfoil-section maximum lift coefficients as high as 5.5 have been obtained in wind-tunnel tests (see, for example, reference 2) and in a limited flight investigation, airplane lift coefficients of 4.2 were obtained (reference 3).

There is, however, some question as to the exact benefits to be obtained by use of the high lift coefficients available with boundary-layer control. In an effort to obtain some idea of the extent to which the high lift coefficients available with boundary-layer control might be useful, an analytical investigation was made of the effect of lift coefficient on the distance required for a liaison type of airplane to take off over a 50-foot obstacle (reference 4).

The investigation reported in reference 4 has recently been extended to include an analysis of the effect of high maximum lift coefficients on the distance required for a liaison type of airplane to land after gliding over a 50-foot obstacle. The results of this analysis are presented in the present paper. The airplane was assumed to have a 1500-pound pay load and to carry enough fuel for a 5-hour flight. The airplane configurations investigated varied in wing span from 25 to 100 feet, in horsepower from 300 to 1200, and had aspect ratios of 5, 10, and 15. Calculations of the landing distance were made in all cases for maximum lift coefficients of 2.8 and 5.0. Allowances were made for changes in the gross weight resulting from variations in plan form, horsepower, and boundary-layer-control equipment. The maximum speed of each airplane configuration was also calculated in order to provide some indication of the relation between high-speed performance and landing distance. The landing manuever was assumed to be executed without the use of engine power.

SYMBOLS

W	airplane gross weight, pounds
w	weight of airplane components, pounds
g	acceleration due to gravity (assumed equal to 32.2), feet per second per second
T	thrust, pounds
T_o	static thrust, pounds
$T_{V_{max}}$	thrust at maximum velocity, pounds
S	wing area, square feet
θ	angle of flight path with respect to ground, degrees
V	velocity, feet per second
$\overline{V}$	average flight velocity during transition arc, feet per second $\left(\frac{V_G + V_s}{2}\right)$
D	total drag, pounds
C_D	airplane drag coefficient (D/qS)
D_o	wing profile drag, pounds
C_{D_o}	wing profile-drag coefficient (D_o/qS)
C_{D_i}	induced drag coefficient $\left(C_L^2/\pi Ae\right)$
L	total lift, pounds
C_L	airplane lift coefficient (L/qS)
C_{L_T}	lift coefficient that would be required for steady level flight at speed $\overline{V}$

$\Delta C_L = C_{L_{max}} - C_{L_T}$

s	horizontal distance, feet
s_L	landing distance from 50-foot obstacle, feet
R	radius of transition arc, feet
q	dynamic pressure, pounds per square foot $\left(\frac{1}{2}\rho V^2\right)$
H	total pressure, pounds per square foot
C_P	pressure coefficient $\left(\frac{H_o - H_d}{q_o}\right)$
Q	quantity rate of flow, cubic feet per second
C_Q	quantity rate of flow coefficient (Q/SV_o)
P	brake horsepower
A	aspect ratio (b^2/S)
h	altitude at which flare is started, feet
b	span, feet
e	wing efficiency factor based on variation of spanwise loading from an elliptical loading with no ground effect (assumed equal to 0.9)
t	wing-root thickness, feet
C	constant for calculating propeller thrust $\left(\frac{T_{V_{max}}}{P}\right)$
η	efficiency factor of blower (assumed equal to 0.9)
μ	combined ground and braking friction coefficient (assumed equal to 0.4)
ρ	mass density of air, slugs per cubic foot

γ	ratio of specific heats at constant volume and constant pressure (1.4 for air)
τ	time, seconds

Subscripts:

c	conventional airplane
BLC	boundary-layer-control airplane
o	free-stream conditions
d	conditions in boundary-layer-control duct
L	conditions at point of ground contact
max	maximum
u	pay load
G	glide
F	float
B	ground
T	transition
s	stalling

METHODS OF ANALYSIS

In calculating the landing performance characteristics, a number of basic assumptions were required for the purpose of determining the airplane configurations, the aerodynamic characteristics, the weight of the complete airplane, and the method used in performing the landing maneuver. The assumptions made for determining the gross weight of the airplane and the aerodynamic characteristics were the same as the assumptions used in the analysis of the airplane take-off characteristics (reference 4). The final comparative results should be unaffected by the assumptions inasmuch as the same assumptions were used for the airplane with boundary-layer control as for the conventional airplane.

Airplane Configuration

The airplane was assumed to have a cantilever semimonocoque wing, rectangular in plan form, with airfoil sections tapering from a thickness ratio of 0.18 at the root to 0.12 at the tip. The empennage area was considered to be 0.25S. The fuselage frontal area F for a pay load w_u of 1500 pounds was determined from the following equation obtained from reference 5:

$$F = 0.15 w_u^{2/3}$$

The dimensions of the fuselage and landing gear remained constant.

The propeller was considered to be fully automatic in order that maximum engine speed and power could be obtained at all airspeeds. The fuel and oil supply was assumed sufficient for 5 hours of cruising at 60 percent of maximum power with a specific fuel consumption of 0.50 pounds per brake horsepower per hour. The engine power available was varied from 300 brake horsepower to 1200 brake horsepower.

It was assumed that an auxiliary engine and a blower were used to apply suction through the duct provided by the internal space of the semimonocoque wing with the boundary-layer-control slots and that the boundary-layer-control apparatus would have a fuel supply sufficient for the flight duration at 60-percent power with a specific fuel consumption of 0.50 pounds per brake horsepower per hour. These conditions should permit continuous operation of the boundary-layer control during flight.

Aerodynamic Characteristics

The variation of wing profile-drag coefficient with wing lift coefficient, shown in figure 1, was determined from section data contained in references 6 to 9. The data are for the smooth-surface condition of the wings with and without boundary-layer control. The use of boundary-layer suction is seen to cause only relatively small changes in the profile drag in the cruising range of lift coefficients. On a wing provided with suction slots to improve the maximum lift, however, suction through these slots must be maintained in the cruising range of lift coefficients in order that the profile drag will not be increased by outflow through the slots. For this reason, the previously mentioned provision of enough fuel to operate the boundary-layer control apparatus continuously during the 5-hour-flight duration was considered necessary. The use of a drag polar based on airfoil-section data for the rough-surface condition would undoubtedly represent a more realistic appraisal of the high-speed characteristics of the airplane configurations investigated. Enough data to permit the determination of the drag polar for

the rough-surface condition were not available, however, at the time that the analysis of reference 4 was made. Since it was considered desirable to make the present analysis comparable with that of reference 4, the same drag polar used in reference 4 for the smooth condition was employed in the present analysis. The assumed empennage drag coefficient based on the empennage area was 0.01 and the assumed fuselage and landing-gear drag coefficients were 0.20 and 0.05, respectively, based on the fuselage frontal area (reference 10). The induced drag coefficients were calculated from the equation

$$C_{D_i} = \frac{C_L^2}{\pi Ae}$$

where the value of e was assumed to be 0.9. The maximum attainable lift coefficients were assumed to be 2.8 and 5.0 for the airplane without and with boundary-layer control, respectively.

Weight Analysis

The gross weight of the airplane can be conveniently expressed in terms of the wing span, aspect ratio, and power. The following equations relating the weight of the airplane to these parameters were obtained from reference 4. The airplane components are designated by the following subscripts:

m	engine
p	propeller, hub, and engine auxiliaries
g	gasoline and oil
F	fuselage
L	landing gear
E	empennage
w	wing
b	blower
bm	blower engine

The weights of the engine, engine auxiliaries, propeller, and hub are given by the following equations:

$$w_m = P\left(\frac{192}{P - 30} + 1.1\right) \tag{1}$$

$$w_p = P\left(\frac{4.58}{P^{0.68}} + 0.48\right) \tag{2}$$

The weight of the gasoline including the required 1 gallon of oil per 16 gallons of fuel for a 5-hour cruise is

$$w_g = 1.62P \tag{3}$$

The empirical relations for the weight of the fuselage, landing gear, empennage, and wing are as follows:

$$w_F = 0.172W^{0.94} \tag{4}$$

$$w_L = 0.067W^{0.98} \tag{5}$$

$$w_E = 0.25S \tag{6}$$

$$w_w = 0.046SA^{0.47}\left(\frac{W}{b}\right)^{0.53}\left(\frac{b}{t}\right)^{0.115} \tag{7}$$

The value of $\frac{b}{t} = 35$ was considered representative for the type of airplane investigated; however, large changes in the ratio of span to root thickness will cause only small changes in the gross-weight estimate inasmuch as the wing weight comprises only about 15 percent of the gross weight and the ratio b/t enters in the wing weight equation to the 0.115 power.

A summation of the aforementioned equations for the weights of the airplane components including 1500 pounds for the pay load w_u yields

the following empirical relation for the gross weight of the assumed conventional airplane as a function of the span, aspect ratio, and horsepower:

$$W_c = P\left(\frac{192}{P - 30} + \frac{4.58}{P^{0.68}} + 3.20\right) + 1500 + 0.172W^{0.94} + 0.067W^{0.98} + S\left[0.25 + 0.07A^{0.47}\left(\frac{W}{b}\right)^{0.53}\right] \quad (8)$$

The gross weight of the airplane with boundary-layer control is then equivalent to the gross weight of the conventional airplane plus the additional weight of the blower engine w_{bm}, blower w_b, and the additional fuel required. The equation for the gross weight of the airplane with boundary-layer control is therefore

$$W_{BLC} = W_c + w_{bm} + w_b \quad (9)$$

The power required by the blower engine can be estimated for a given compression ratio, flow quantity, absolute entrance pressure, and blower efficiency by means of the following expression for an adiabatic gas flow:

$$P_{bm} = \frac{\frac{\gamma}{\gamma - 1}H_d Q}{550\eta}\left[\left(\frac{H_o}{H_d}\right)^{\frac{\gamma-1}{\gamma}} - 1\right] \quad (10)$$

The results presented in reference 3 indicate that adequate boundary-layer control for a maximum lift coefficient of 5.0 can be obtained with a flow coefficient C_Q of 0.03 and a pressure coefficient C_P of 4.0. In order to make a conservative estimate of the weight of the boundary-layer control equipment, however, a flow coefficient of 0.04 and a pressure coefficient of 15 were assumed. (See reference 11.) Substitution of the assumed values of C_P and C_Q in

equation (10) results in the following equation for an assumed blower efficiency of 0.9:

$$P_{bm} = 0.00367\left(H_o - 3\frac{W}{S}\right)\sqrt{WS}\left[\left(\frac{H_o}{H_o - 3\frac{W}{S}}\right)^{0.286} - 1\right] \qquad (11)$$

Assumption of an engine weight of 2.5 pounds per horsepower and fuel for 5 hour duration at 60-percent power results in the following equation for the weight of the blower engine and fuel:

$$w_{bm} = 4P_{bm} = 0.0147\left(H_o - 3\frac{W}{S}\right)\sqrt{WS}\left[\left(\frac{H_o}{H_o - 3\frac{W}{S}}\right)^{0.286} - 1\right] \qquad (12)$$

In order that the blower weight could be determined, the blower was assumed to be an axial-flow stator-rotor type constructed of aluminum alloy and having a hub-to-tip ratio of 0.6 and an axial velocity of 400 feet per second. The outer casing was assumed to be 0.125 inch thick and 48 inches long. The rotor, blades, and shaft were considered equivalent to a disk 2 inches thick with a diameter 0.8 of the tip diameter; whereas the stator vanes were considered equivalent to a disk having a thickness of 0.25 inch and the same diameter as that of the complete rotor. The blower weight equation was developed from these assumptions and is as follows

$$w_b = 0.044\sqrt{WS} + 1.13(WS)^{0.25} \qquad (13)$$

Landing Maneuver

The landing maneuver was considered to consist of four phases: the steady glide, a transition path executed at maximum lift coefficient to bring the airplane from a steady glide to level flight, a floating period of 2 seconds to allow for lag in control response and for the application of brakes (see reference 12), and finally the ground run. The beginning of the landing was considered as the point at which the altitude was 50 feet; the total landing distance was considered to be the horizontal distance from this point to the end of the ground run. The maneuver was considered to be performed without the use of power,

that is, no propeller drag or thrust, and with no wind. A sketch illustrating the assumed maneuver is presented in figure 2.

Basic assumptions.- In calculating the total landing distance, certain simplifying assumptions were made in connection with the manner in which the transition from the steady-glide speed and attitude to level-flight speed and attitude was executed. These assumptions were based on the concept that the horizontal distance covered during the transition period for the type of airplane considered is a relatively small portion of the total landing distance so that a precise determination of the transition path is not required. The simplifying assumptions were:

1. The airplane was assumed to execute the transition at maximum lift coefficient and the transition path was assumed to be represented by an arc of constant radius. This assumption implies, of course, a constant speed during the transition.

2. Although a constant speed was assumed for the transition arc, it is, of course, obvious that in the actual case the speed during the transition must vary from the steady-glide speed to the landing speed. The constant speed implied by the assumption of a transition arc of constant radius was determined by assuming a linear variation in speed from the steady-glide speed to the stalling speed and taking the constant speed as the arithmetic mean of these two values. This assumption implies a constant decelerating force during the transition.

These assumptions are somewhat similar to those found in approximate methods for calculating the transition path following take-off (reference 13). Such approximate methods for calculating the take-off distance have been found to give good results and, in those cases for which experimental data were available, the method outlined for calculating the landing distance was also found to give good results.

Development of landing equations.- On the basis of assumptions 1 and 2 the following equations for the total landing distance can be derived. The horizontal distance covered during the transition arc s_T is considered first. Reference to figure 2 shows that

$$s_T = R \sin \theta_G \tag{14}$$

where θ_G is the angle of steady glide and R is the radius of the transition arc. The instantaneous radius of curvature during a pull-up at maximum lift is given by the expression:

$$R = \frac{2}{\rho g} \frac{W}{S} \frac{1}{C_{L_{max}} - C_{L_T} \cos \theta} \tag{15}$$

where C_{L_T} in this equation corresponds to the lift coefficient for unaccelerated level flight at the velocity at which the pull-up is being executed and θ is the instantaneous flight-path angle. If the cosine of the glide-path angle is assumed to be 1.0, equation (15) can be written as follows:

$$R = \frac{2}{\rho g} \frac{W}{S} \frac{1}{\Delta C_L} \tag{16}$$

where ΔC_L is the difference between the maximum lift coefficient and the lift coefficient corresponding to the previously defined mean speed used during the transition. Since the stalling speed is known, the value of the steady-glide speed V_G is all that is required for the determination of R and the horizontal distance covered during the transition. The value of V_G must be chosen in such a way that the time required for the velocity to decrease from V_G to V_L is the same as the time required for the airplane to traverse the distance s_T. The tangential forces acting on the airplane during the transition arc are composed of the drag which is a decelerating force and the component of weight along the flight path which is an accelerating force. The mean decelerating drag force D_T is determined from the drag coefficient at the maximum lift coefficient and the mean speed $\overline{V}$.

There is, however, an accelerating force which may be determined in the following manner. At the end of the steady glide the following relation holds:

$$D_G = W \sin \theta_G$$

where D_G is the drag in the steady glide. Since the glide angle θ_G is usually small, θ varies in a nearly linear manner with s_T during the transition, and since $\sin \theta$ also varies in a nearly linear manner with θ for small values of θ, the mean accelerating force during the transition may be written as

$$\frac{W \sin \theta}{2} = \frac{D_G}{2}$$

Therefore, the time required for the airplane to decelerate from the steady glide speed V_G to the landing speed V_L is then given by the following expression:

$$\tau = \frac{W}{g} \frac{V_G - V_L}{D_T - \frac{D_G}{2}} \tag{17}$$

If the cosine of the flight-path angle is considered to be unity, the time required to traverse the distance s_T is

$$\tau = \frac{s_T}{\overline{V}} \tag{18}$$

where $\overline{V}$ is the mean speed. Since the two intervals of time expressed by equations (17) and (18) must be equal, the distance s_T may be expressed in the following form

$$s_T = \frac{2\overline{V}\left(V_G - V_L\right)W}{g\left(2D_T - D_G\right)} \tag{19}$$

If

$$\sin \theta_G = \sin \tan^{-1}\left(\frac{C_D}{C_L}\right)_G = \left(\frac{C_D}{C_L}\right)_G$$

the distance s_T as given by equations (14) and (16) may be written

$$s_T = \frac{2}{\rho g} \frac{W}{S} \frac{1}{\Delta C_L}\left(\frac{C_D}{C_L}\right)_G \tag{20}$$

A simultaneous solution of equations (19) and (20) gives, after some algebraic manipulation, the following equation:

$$\left[\left(\frac{C_D}{C_L}\right)_L\left(\frac{C_D}{C_L}\right)_G - 6\right]\left(\frac{V_L}{V_G}\right)^3 + \left[3\left(\frac{C_D}{C_L}\right)_G\left(\frac{C_D}{C_L}\right)_L + 10\right]\left(\frac{V_L}{V_G}\right)^2 +$$

$$\left[\left(3 - 2\frac{C_{D_G}}{C_{D_L}}\right)\left(\frac{C_D}{C_L}\right)_G\left(\frac{C_D}{C_L}\right)_L - 2\right]\left(\frac{V_L}{V_G}\right) +$$

$$\left[\left(1 - 2\frac{C_{D_G}}{C_{D_L}}\right)\left(\frac{C_D}{C_L}\right)_G\left(\frac{C_D}{C_L}\right)_L - 2\right] = 0 \qquad (21)$$

An exact solution of equation (21) for $\frac{V_L}{V_G}$ requires additional analytic expressions relating $\left(\frac{C_D}{C_L}\right)_G$ and $\frac{C_{D_G}}{C_{D_L}}$ to $\frac{V_L}{V_G}$. Such relations can, of course, be found by expressing the drag polars for the various airplanes in analytic form. It was found more convenient, however, to perform a simultaneous solution of equations (19) and (20) by a trial and error process. Once the correct value of V_G is determined from equations (19) and (20), the horizontal distance covered in the transition arc is easily calculated for a particular airplane from equation (20).

The horizontal distance s_G, covered in the steady glide from a height of 50 feet to the height h at which the transition is begun can be calculated by the following equations (see fig. 2):

$$s_G = \frac{50 - h}{\tan \theta_G} = \frac{50 - h}{\left(\frac{C_D}{C_L}\right)_G}$$

but

$$h = R\left(1 - \cos \theta_G\right)$$

so that

$$s_G = \frac{50 - R\left[1 - \cos \tan^{-1}\left(\frac{C_D}{C_L}\right)_G\right]}{\left(\frac{C_D}{C_L}\right)_G} \tag{22}$$

The values of R and $\left(\frac{C_D}{C_L}\right)_G$ are already known from the previous calculations of the transition path so that s_G may be readily determined. The distance covered during the floating period is merely

$$s_F = 2V_L = 2\sqrt{\frac{2W}{\rho S C_{L_{max}}}} \tag{23}$$

The equation for determining the ground run or braking distance, obtained from reference 14, is

$$s_B = \frac{V_L^2}{2g\left(\frac{C_D}{C_L} - \mu\right)} \log_e \left(\frac{C_D/C_L}{\mu}\right) \tag{24}$$

where $\frac{C_D}{C_L}$ is the lift-drag ratio for the maximum-lift condition and V_L corresponds to the stalling speed. The combined ground and braking friction coefficient was assumed to be 0.4. This value of the friction coefficient can be obtained with cinders on ice. (See reference 12.) The ground effect on the induced drag was neglected. The total landing distance is obtained from a summation of the horizontal distances covered during the four phases of the maneuver:

$$s_L = s_G + s_T + s_F + s_B$$

where these four components are calculated by means of equations (22), (20), (23), and (24), respectively.

Maximum Speed

The method employed for calculating the maximum speed of the various airplane configurations was the same as that used in reference 4. This method was originally developed in reference 13 and can be briefly described as follows: The thrust at the maximum speed can be expressed as

$$T_{V_{max}} = \frac{P550\eta_P}{V_{max}}$$

where η_P is the propulsive efficiency. Airplanes having various combinations of power and maximum speed were investigated in reference 13 and the thrust at maximum velocity was found to be, if propellers having the optimum diameter and blade setting for a particular maximum speed are employed,

$$T_{V_{max}} = CP \tag{25}$$

where C is a linear function of the maximum velocity. The functional relation between V_{max} and C as expressed in reference 4 is

$$C = 3.09 - 0.005V_{max} \tag{26}$$

The thrust at maximum velocity can also be expressed as

$$T_{V_{max}} = \frac{1}{2}\rho V_{max}^2 \frac{b^2}{A} C_D \tag{27}$$

where C_D is the summation of the assumed drags of the airplane components in coefficient form. With the use of the three expressions, equations (25), (26), and (27), the following relation for the maximum velocity is obtained

$$P\left(3.09 - 0.005V_{max}\right) = \frac{1}{2}\rho V_{max}^2 \frac{b^2}{A} C_D \tag{28}$$

Equation (28) was employed for calculating the maximum velocity of the various airplanes.

SCOPE OF CALCULATIONS

The airplanes for which the total landing distance was calculated had wing spans varying from 25 feet to 100 feet, engine brake horsepowers varying from 300 to 1200, and aspect ratios of 5, 10, and 15. As previously stated, the wing span, aspect ratio, and power determine the weight of an airplane, and the airplane configuration. The landing distance was calculated for each airplane with and without boundary-layer control. The maximum lift coefficient of the airplane with boundary-layer control was assumed to be 5.0 and that of the airplane without boundary-layer control was assumed to be 2.8. Data defining the range of airplane configurations for which the performance calculations were made are presented in figures 3 and 4 for the airplanes without and with boundary-layer control, respectively. The weights as calculated from equations (8) and (9) resulted in wing loadings of the airplanes investigated which varied from about 4 pounds per square foot to about 160 pounds per square foot for the airplanes without boundary-layer control and from about 4 pounds per square foot to about 180 pounds per square foot for the airplanes with boundary-layer control. The maximum velocity of the different airplane configurations with and without boundary-layer control was calculated so as to provide a basis of comparison for the high- and low-speed performance and is given in figure 5. For a given wing span, aspect ratio, and brake horsepower of the main propulsive unit, the maximum velocities of the airplanes with and without boundary-layer control differ only to the extent to which the weight of the boundary-layer control equipment alters the wing loading and thus the drag coefficient at any given speed and to the small extent to which the drag polars of the airplanes with and without boundary-layer control differ.

RESULTS AND DISCUSSION

The power-off landing performance characteristics to be discussed are:

(1) the total landing distance
(2) the ground-run distance
(3) the speeds at which the different phases of the landing maneuver are executed

The discussion is intended to show the relative effect of increasing the maximum lift coefficient by boundary-layer control upon these performance characteristics and upon the relation between high-speed performance and landing performance as the airplane configuration is varied. The pertinent landing-performance characteristics are presented

in terms of the wing span, power, and aspect ratio for the airplanes with and without boundary-layer control. The choice of variables employed in presenting the data was arbitrary to some extent. Although other parameters could have been employed, span, aspect ratio, and power were chosen because these variables indicate the physical size and practicability of the airplane. In some cases, the performance parameters were plotted against wing loading as well as wing span because the use of the wing loading in these cases tended to clarify the results.

Total Landing Distance

The total landing distance is presented as a function of wing span in figure 6 with power as the parameter. The data are for aspect ratios of 5, 10, and 15 and are for the airplanes with and without boundary-layer control. An examination of the data of figure 6 indicates that, for a given engine power and aspect ratio, the landing distance decreases rapidly with increasing span over a certain range of spans, after which further increases in span have little effect. This is a result of the manner in which the wing loading varies with span. (See figs. 3 and 4.) For a given wing span, the landing distance is seen to increase with increasing engine power. In all cases, increasing the apsect ratio for a fixed span and power increases the total landing distance. For any given aspect ratio, the shortest landing distance is obtained for the airplane with largest span and lowest power. These trends are evident in the data for all three aspect ratios and for the airplanes with and without boundary-layer control. The effect of boundary-layer control on the total landing distance can best be seen in figure 7. In this figure the ratio of the total landing distance with boundary-layer control to the total distance without boundary-layer control is plotted as a function of span. The data clearly indicate that, regardless of engine power or aspect ratio, the use of maximum lift coefficients of the order of 5.0 which can be obtained only with boundary-layer control as compared with lift coefficients of 2.8 which can be obtained without boundary-layer control results in decreases in the total landing distance which vary between 25 and 40 percent. The largest percentage decrease occurs for the rather unconventional airplane configuration with 1200 horsepower, a 25-foot span, and an aspect ratio of 10.

The data of figure 8 show that, for a constant wing loading, the use of boundary-layer control results in reductions of the total landing distance which vary from about $27\frac{1}{2}$ to $43\frac{1}{2}$ percent. The slightly more favorable effect of boundary-layer control when the comparison is based on a constant wing loading rather than on a constant span is explained by the fact that the addition of boundary-layer control to the airplane of constant span increases the wing loading by a small amount which has

an adverse effect on the landing distance. For a constant wing loading, variations in the engine power have a negligible effect upon the landing distance (fig. 8); hence, the relatively large adverse effect of increasing the power upon the landing distance of an airplane of constant span, shown by the data of figure 6, results from the effect of engine power on wing loading. It might also be thought that the adverse effect upon the landing distance of increasing the aspect ratio for a given span and power (fig. 6) could be attributed entirely to an increase in wing loading. The data of figure 8, however, show that for a given wing loading, increasing the aspect ratio also causes some increase in the landing distance. This unfavorable effect of increasing aspect ratio on the landing distance results from the fact that as the aspect ratio is increased the airplane lift-drag ratio is also increased so that there results a flatter glide and, hence, a greater horizontal distance from the 50-foot obstacle to the point of ground contact. The proper application of a spoiler or air brake might, therefore, reduce or eliminate the unfavorable effect of increasing aspect ratio on the total landing distance.

The over-all conclusion to be drawn from the data of figures 6 to 8 is that boundary-layer control causes a substantial reduction in the total landing distance of all the airplane configurations investigated. The minimum landing distance for the configurations investigated was obtained for the airplane configuration having boundary-layer control and the lowest wing loading and aspect ratio, that is a wing loading of 4 pounds per square foot, and an aspect ratio of 5.

As previously pointed out, an airplane is seldom designed in terms of only one performance parameter. An examination of the data of figure 5 indicates that for a given wing span and engine power, the application of boundary-layer control does not have any appreciable effect upon the maximum speed. Consequently, the reductions in landing distance resulting from boundary-layer control (figs. 6 to 8) can be obtained without any sacrifice in maximum speed in most cases. In order to show this effect more clearly, the total landing distance has been plotted against maximum speed in figure 9 for the airplanes with and without boundary-layer control. Figure 9 shows that for a given maximum speed the use of boundary-layer control results in a 25 to 40 percent decrease in the landing distance. The wing spans of the different airplanes are indicated by symbols on these curves. It is interesting to note that for most cases large increases in the maximum speed can be obtained with no increase in the landing distance by the use of boundary-layer control along with reduction in span. The unfavorable effect of increasing aspect ratio on the landing distance for a given maximum speed is, as previously pointed out, a result of the higher lift-drag ratio of the airplanes of high aspect ratio. The fact that boundary-layer control does not have a favorable effect upon the landing distance for the highest maximum speeds obtainable with a given power is explained by the

data of figure 5 which show that the highest possible speed for a given power is slightly higher for the airplane without boundary-layer control than for the airplane with boundary-layer control.

The data presented in figures 6 to 9 lead to the conclusion that the high lift coefficients available with boundary-layer control are very effective in reducing the landing distance of the type of airplane considered in this investigation. A somewhat different conclusion was reached in reference 4 with respect to the effect on the total take-off distance of the increased lift coefficients available with boundary-layer control. The data of reference 4 showed that there was no appreciable decrease in the total take-off distance due to boundary-layer control for a given maximum speed unless the aspect ratio was of the order of 15 and that the minimum total take-off distance for the configurations investigated occurs for aspect ratios of 10 to 15. Even for the higher aspect ratios, the relative effect of boundary-layer control on the total take-off distance is small as compared to its effect on the landing distance.

Ground-Run Distance

In some cases the ground-run distance may be of considerable importance. The ground-run distance is plotted against wing span for different aspect ratios and engine horsepowers in figure 10 and against maximum speed in figure 11. The data of figure 10 indicate that the use of boundary-layer control results in reductions of the ground-run distance which vary from 30 to 40 percent depending upon the configuration. The use of the lowest possible wing loading, that is, low aspect ratio and engine of low power, gives the shortest ground-run distance for a given span.

The data of figure 11 indicate that, for nearly all configurations, reductions in the ground-run distance of 35 to 40 percent can be obtained by the use of boundary-layer control without compromising the maximum speed. In comparison with the trends of figure 11, the data of reference 4 indicate that boundary-layer control has an important effect upon the ground run to take-off for a given maximum speed only if the aspect ratio is of the order of 10 to 15 and that the ground run for take-off is generally longer than that for landing.

Landing Speeds

The speeds with which the various phases of the landing maneuver are executed are of some importance as an indication of the piloting skill required to land a particular airplane. For this reason, data

are given in figures 12 to 14 pertaining to the effect of boundary-layer control on the stalling speed, vertical speed in the steady glide, and steady glide speed.

Stalling speed.- The stalling speed of an airplane is often considered to be of importance and the relation between the maximum speed and the stalling speed to be a significant criterion of airplane performance. The stalling speed of the various airplane configurations with and without boundary-layer control is plotted in figure 12 against the maximum speed. The data of figure 12 show that, unless very high speeds are required for a given aspect ratio and power, the use of boundary-layer control causes reductions in the stalling speed for a given maximum speed of the order of 20 to 25 percent.

Sinking speed and steady glide speed.- The effect of boundary-layer control on the sinking speed is shown in figure 13 where the vertical velocity is plotted against wing span for various horsepowers and aspect ratios for the airplanes with and without boundary-layer control. The data show that boundary-layer control has only a relatively small effect on the sinking speed in all cases. For all the airplanes both with and without boundary-layer control, reducing the span for a given aspect ratio and engine power is seen to increase the sinking speed.

In figure 14 the velocity in the steady glide is plotted against wing span for the airplanes of different aspect ratio and power both with and without boundary-layer control. In all cases, the use of boundary-layer control is seen to reduce the speed in the steady glide by 20 to 25 percent. As would be expected, the steady-glide speed increases with decreasing span for a fixed power and aspect ratio in all cases. Increasing the aspect ratio for a given span and power also increases the gliding speed because of the associated increase in wing loading.

CONCLUSIONS

An analysis was made to determine the effect of boundary-layer control on the landing-performance characteristics, power off, of an assumed liaison type of airplane having aspect ratios ranging from 5 to 15, wing spans ranging from 25 to 100 feet, and engine brake horsepowers ranging from 300 to 1200. The airplanes had a 1500-pound pay load and a cruising duration of 5 hours. The results of the analysis indicate the following conclusions:

1. For a specified airplane maximum speed, the total landing distance can be reduced from 25 to 40 percent by the use of boundary-layer

control. The ground-run distance for a given maximum speed can be reduced 30 to 40 percent by the use of boundary-layer control.

2. A comparison of the results presented with those of a previous analysis of the effect of boundary-layer control on the take-off distance shows that boundary-layer control is much more effective in reducing the landing distance than the take-off distance.

3. The gliding and stalling speeds were 20 to 25 percent lower for most of the airplanes with boundary-layer control than for the airplanes without boundary-layer control.

4. For a fixed wing span, the sinking speed, or vertical velocity, was slightly higher for the airplane with boundary-layer control than for the conventional airplane.

Langley Aeronautical Laboratory
National Advisory Committee for Aeronautics
Langley Air Force Base, Va., May 9, 1950

REFERENCES

1. Hagerman, John R.: Wind-Tunnel Investigation of the Effect of Power and Flaps on the Static Lateral Stability and Control Characteristics of a Single-Engine High-Wing Airplane Model. NACA TN 1379, 1947.

2. Regenscheit, B.: Hochauftriebsversuche mit Absaugeklappenflügeln. Bericht A64 der LGL, 1938, pp. 27-34.

3. Stüper: Flight Experiences and Tests on Two Airplanes with Suction Slots. NACA TM 1232, 1950.

4. Horton, Elmer A., and Quinn, John H., Jr.: Analysis of the Effects of Boundary-Layer Control on the Take-Off Performance Characteristics of a Liaison-Type Airplane. NACA TN 1597, 1948.

5. Ivey, H. Reese, Fitch, G. M., and Schultz, Wayne F.: Performance Selection Charts for Gliders and Twin-Engine Tow Planes. NACA MR L5E04, 1945.

6. Abbott, Ira H., Von Doenhoff, Albert E., and Stivers, Louis S., Jr.: Summary of Airfoil Data. NACA Rep. 824, 1945.

7. Schrenk, Oskar: Experiments with a Wing from Which the Boundary Layer is Removed by Suction. NACA TM 634, 1931.

8. Quinn, John H., Jr.: Tests of the NACA 65_3-018 Airfoil Section with Boundary-Layer Control by Suction. NACA CB L4H10, 1944.

9. Quinn, John H., Jr.: Wind-Tunnel Investigation of Boundary-Layer Control by Suction on the NACA 65_3-418, a = 1.0 Airfoil Section with a 0.29-Airfoil-Chord Double Slotted Flap. NACA TN 1071, 1946.

10. Wood, Karl D.: Airplane Design.. Fourth ed., Cornell Co-Op Soc., Ithaca, N.Y., June 1939.

11. Krüger, W.: Calculations and Experimental Investigations on the Feed-Power Requirement of Airplanes with Boundary-Layer Control. NACA TM 1167, 1947.

12. Gustafson, F. B.: Tire Friction Coefficients and Their Relation to Ground-Run Distance in Landing. NACA ARR, June 1942.

13. Wetmore, J. W.: Calculated Effect of Various Types of Flap on Take-Off over Obstacles. NACA TN 568, 1936.

14. Diehl, Walter Stuart: Engineering Aerodynamics. The Ronald Press Co., rev. ed., 1936, p. 447.

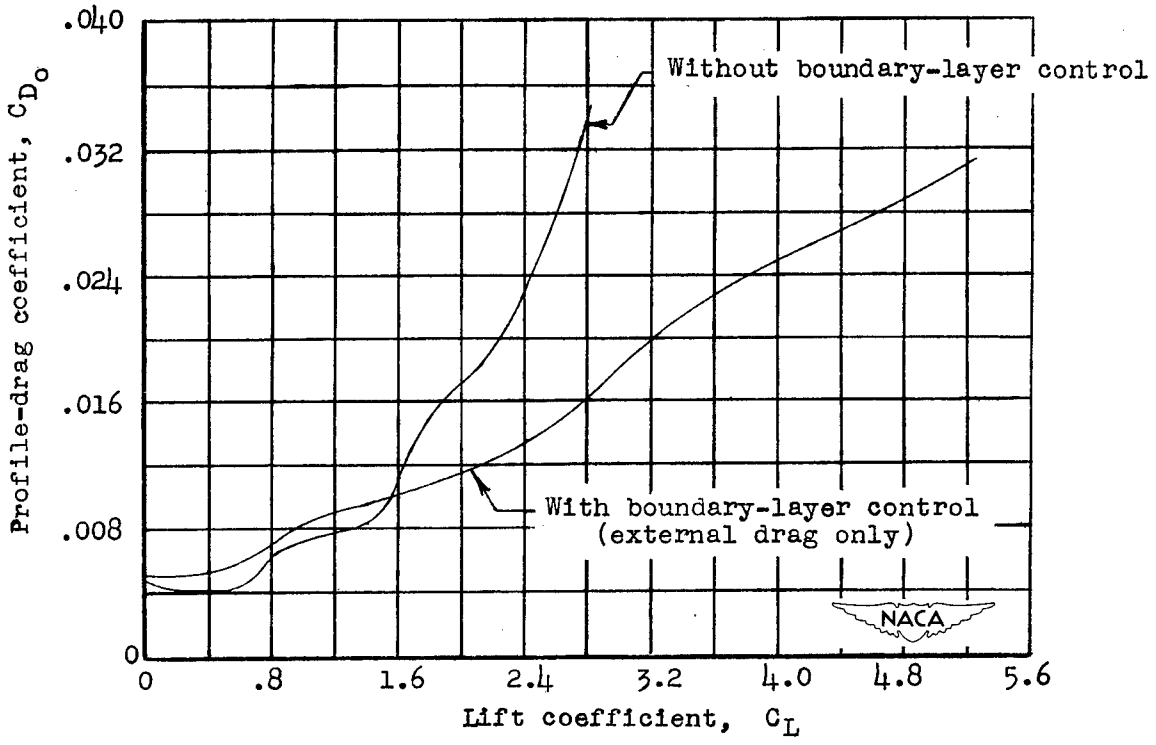

Figure 1.- Assumed profile-drag coefficient of the wing with and without boundary-layer control.

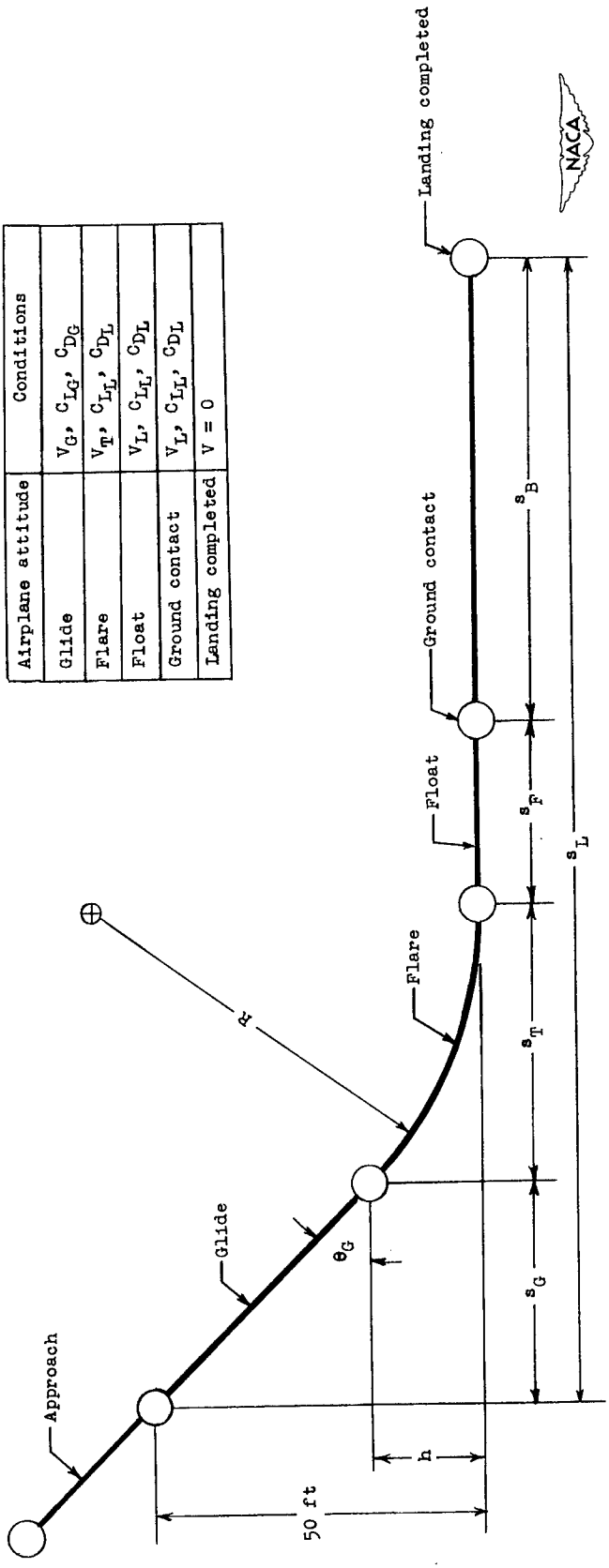

Figure 2.- Illustration of assumed maneuver to clear a 50-foot obstacle in landing.

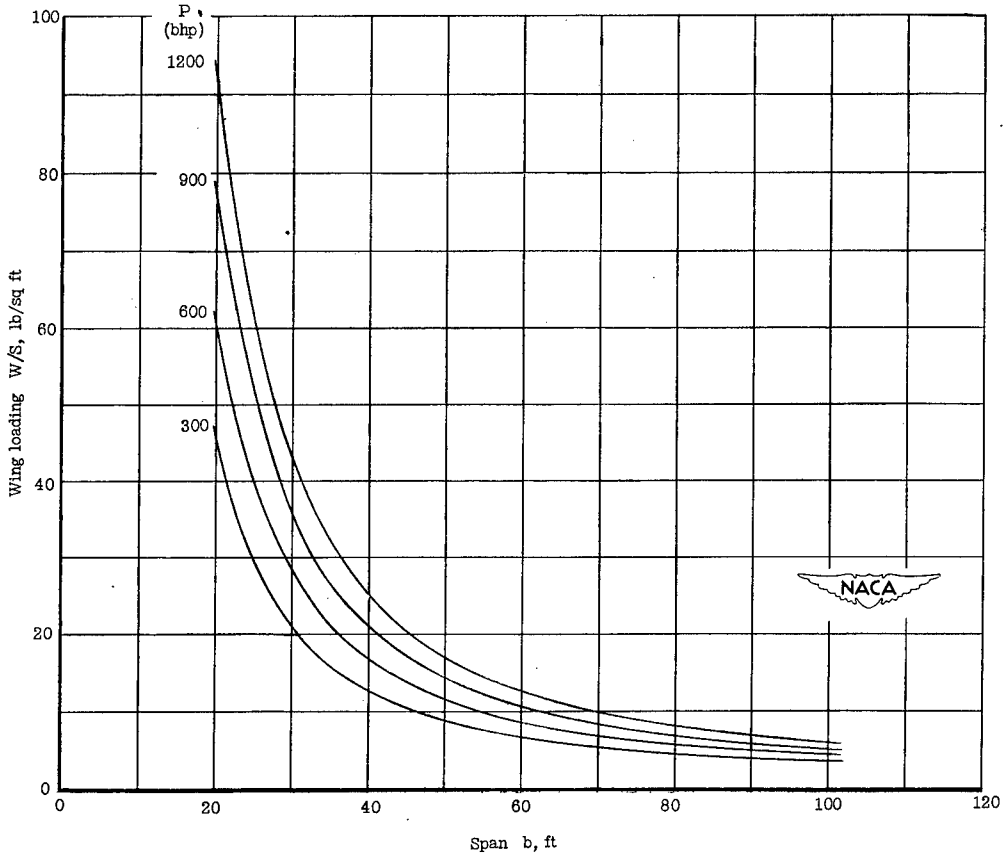

(a) A = 5.

Figure 3.- Wing loading of assumed airplane without boundary-layer control as a function of span for various powers.

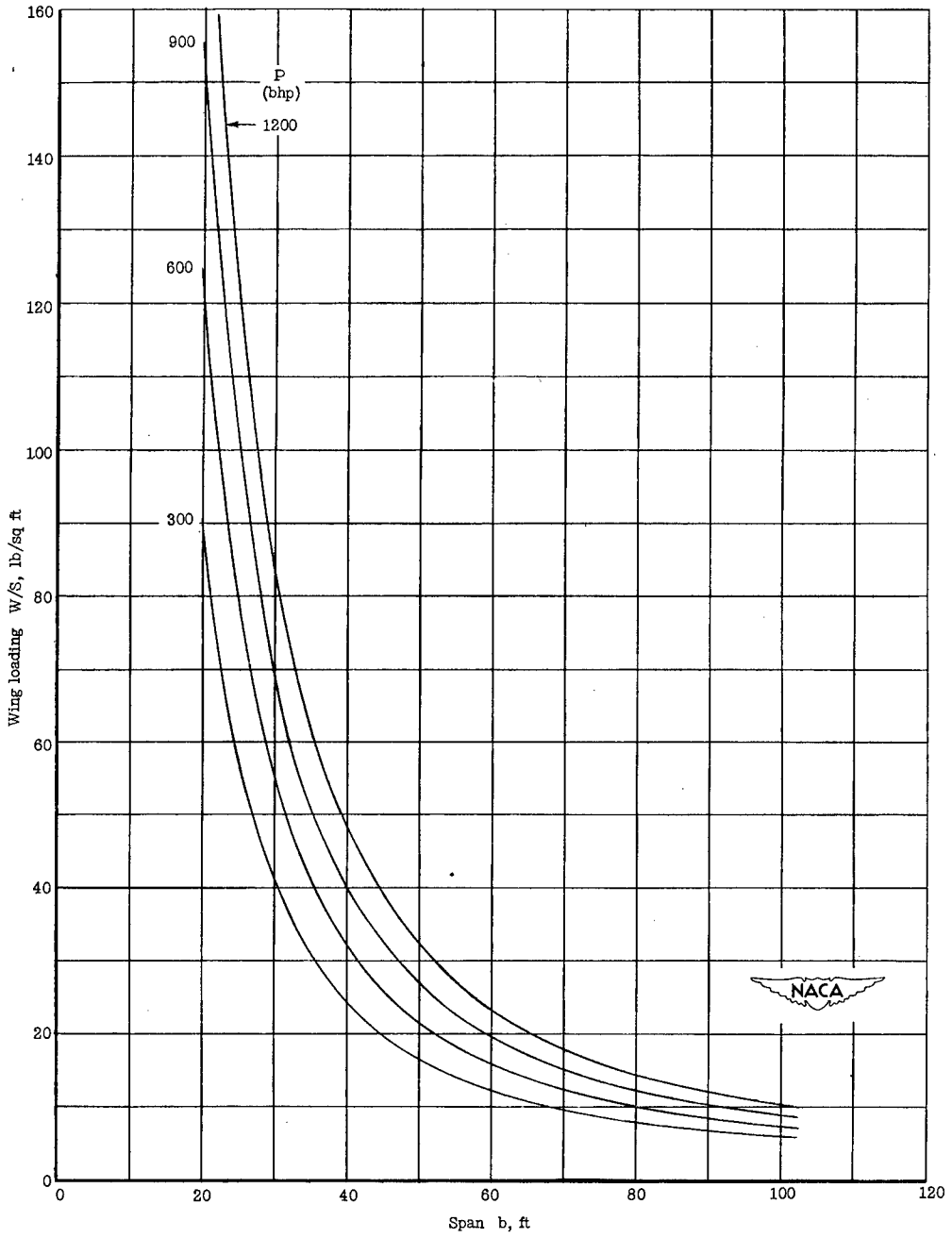

(b) A = 10.

Figure 3.- Continued.

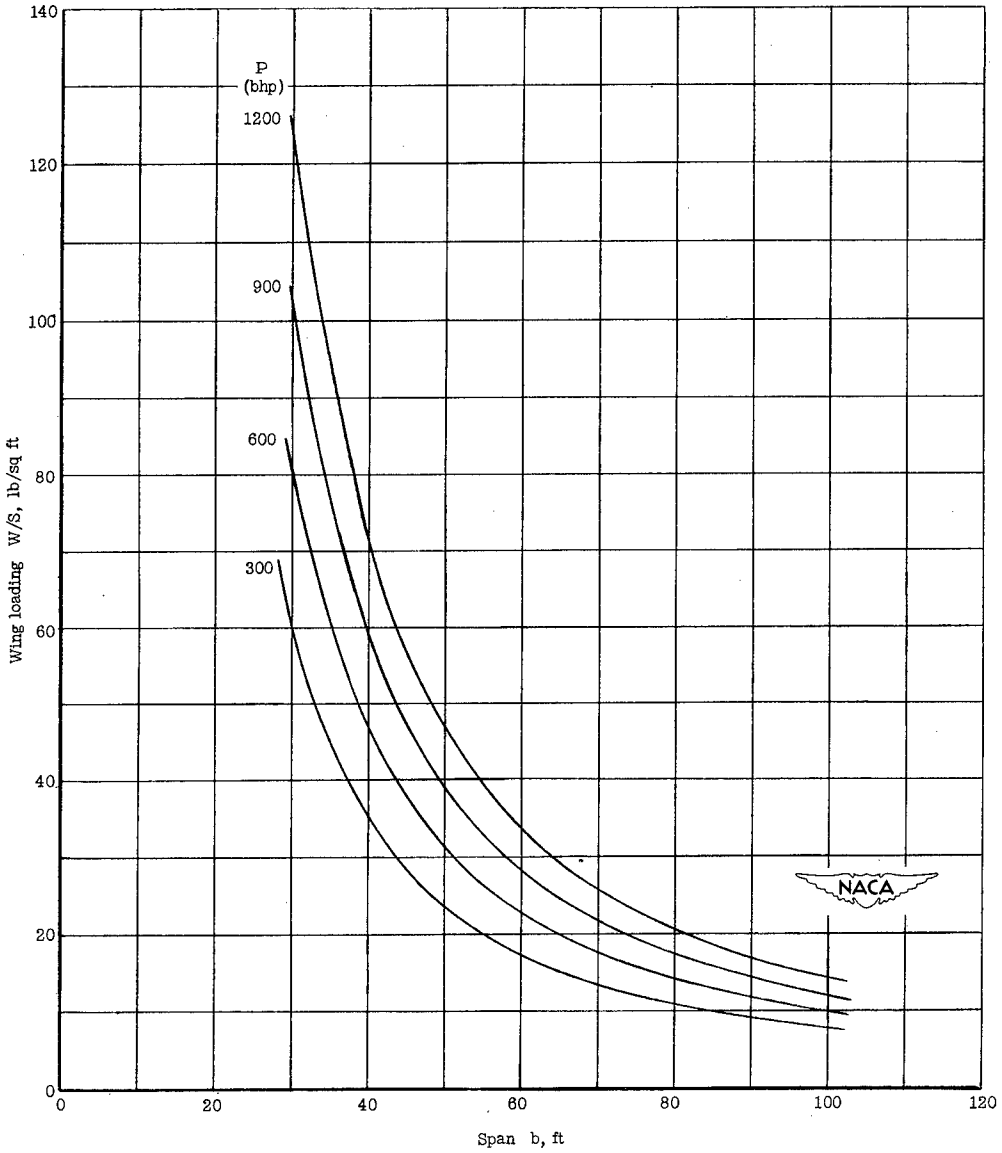

(c) A = 15.

Figure 3.- Concluded.

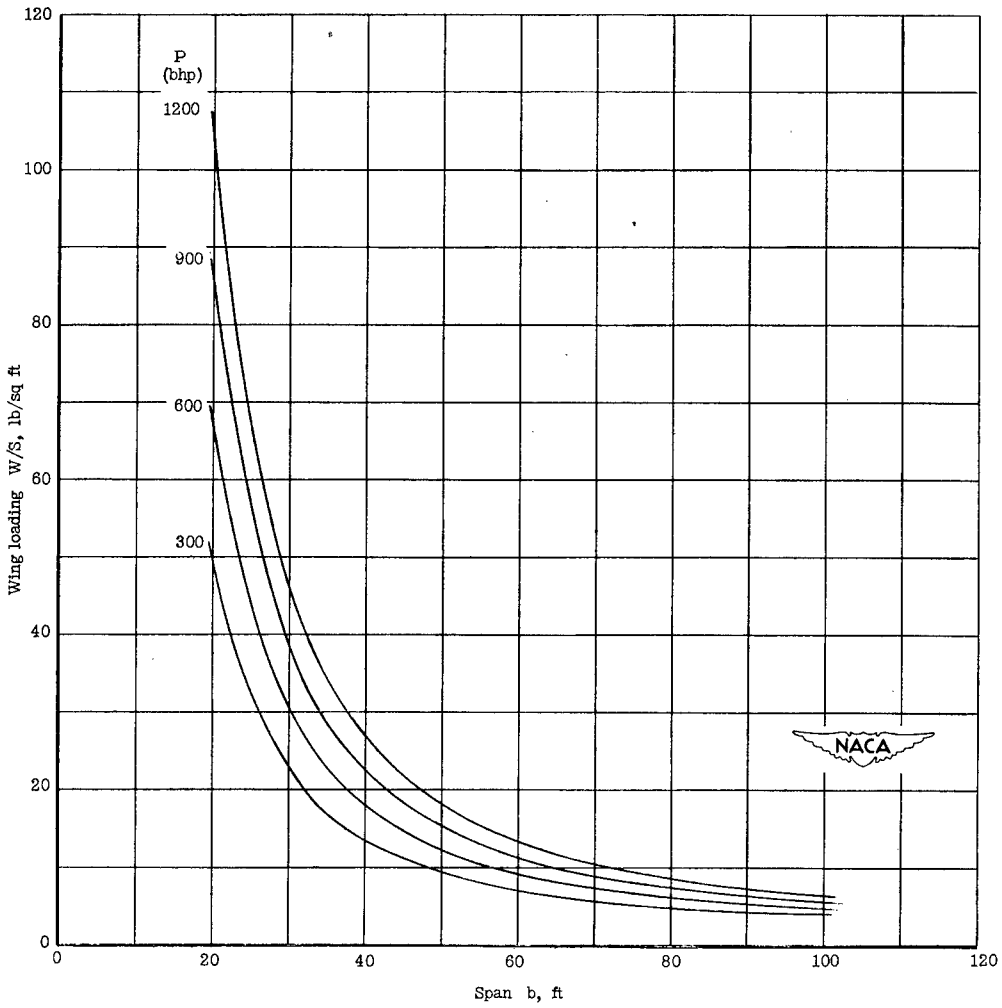

(a) A = 5.

Figure 4.- Wing loading of assumed airplane with boundary-layer control as a function of span for various powers.

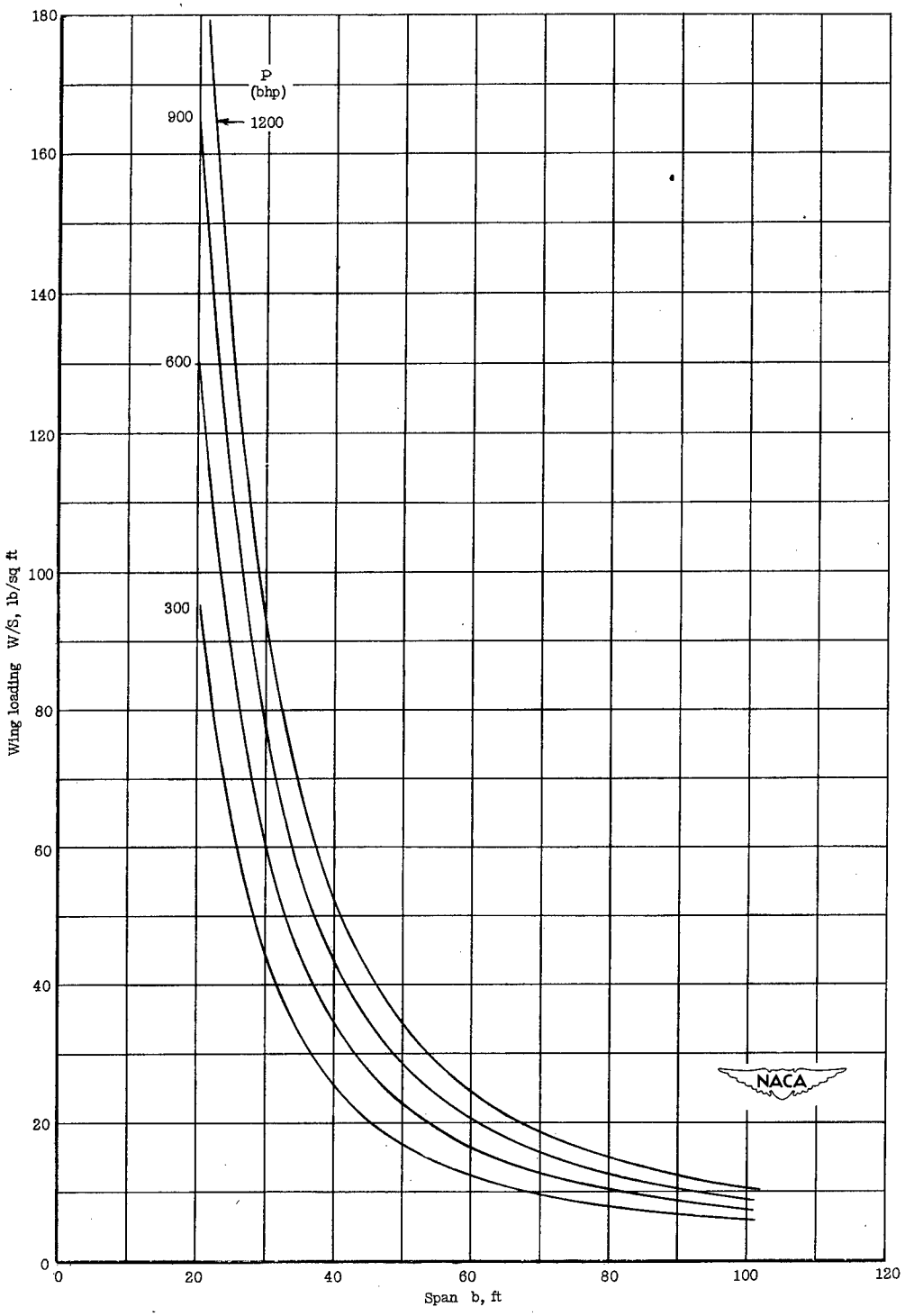

(b) A = 10.

Figure 4.- Continued.

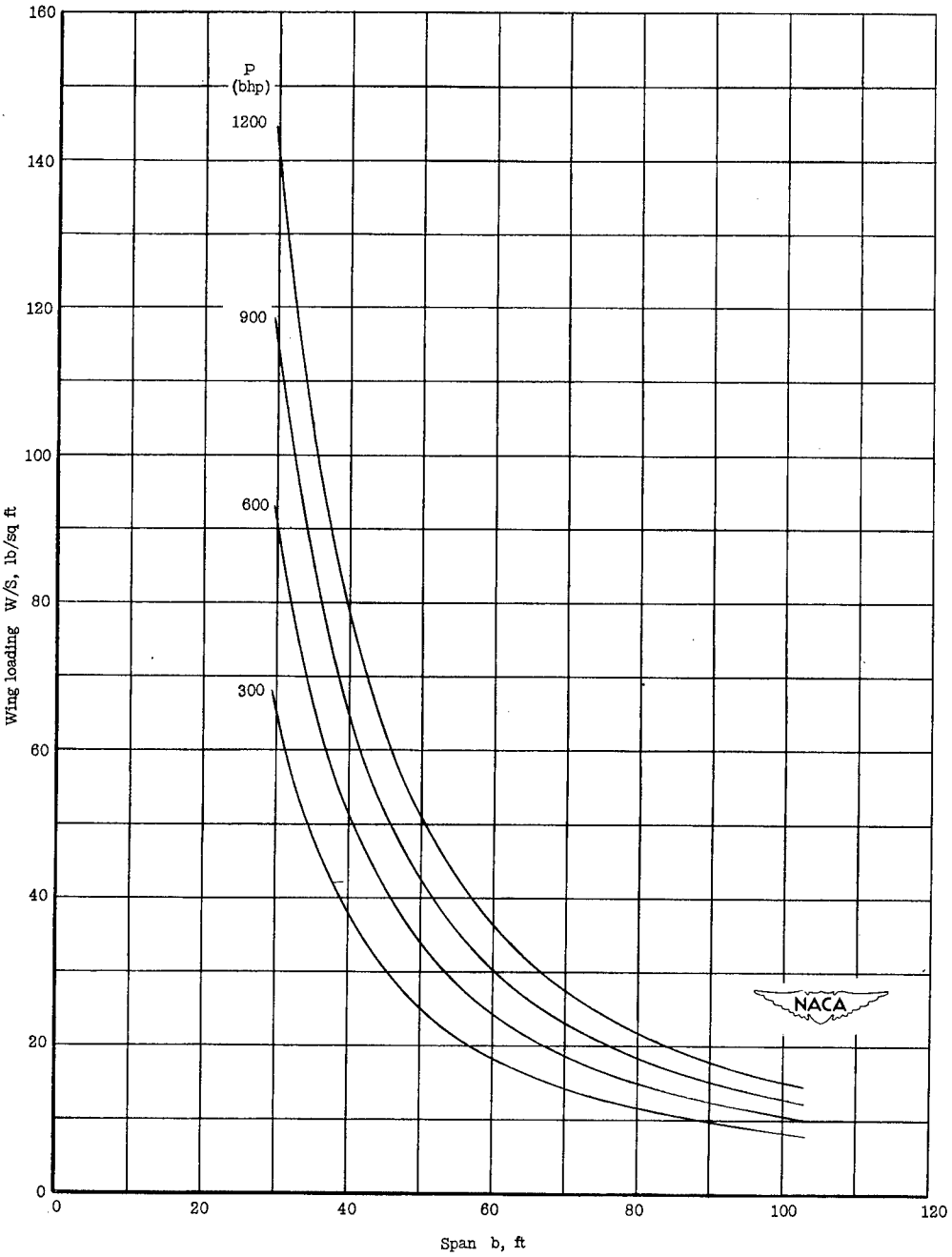

(c) A = 15.

Figure 4.- Concluded.

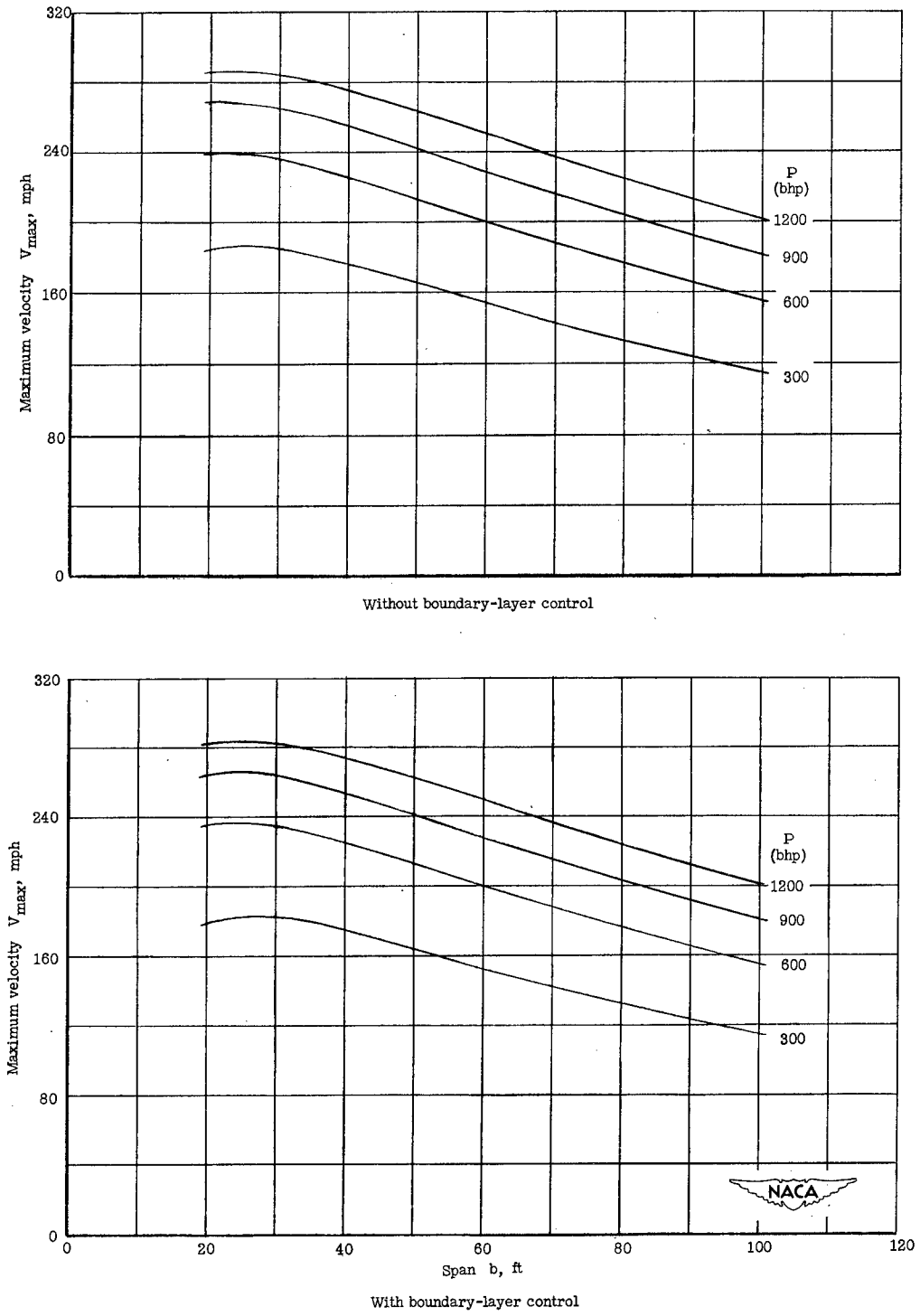

(a) A = 5.

Figure 5.- Maximum velocity of assumed airplane with and without boundary-layer control as a function of span for various powers.

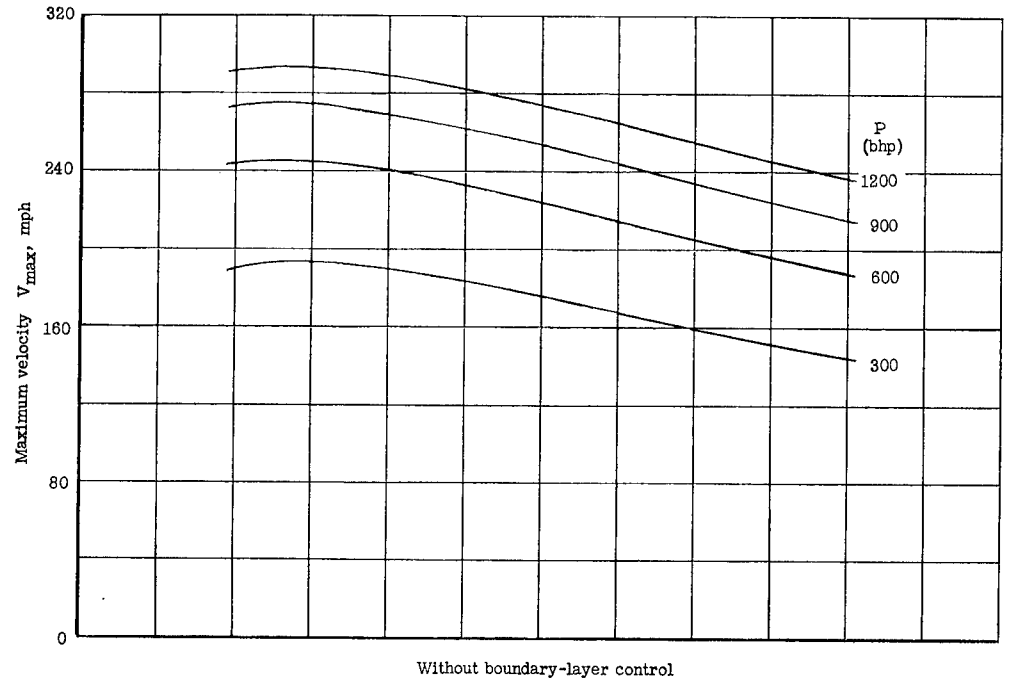

Without boundary-layer control

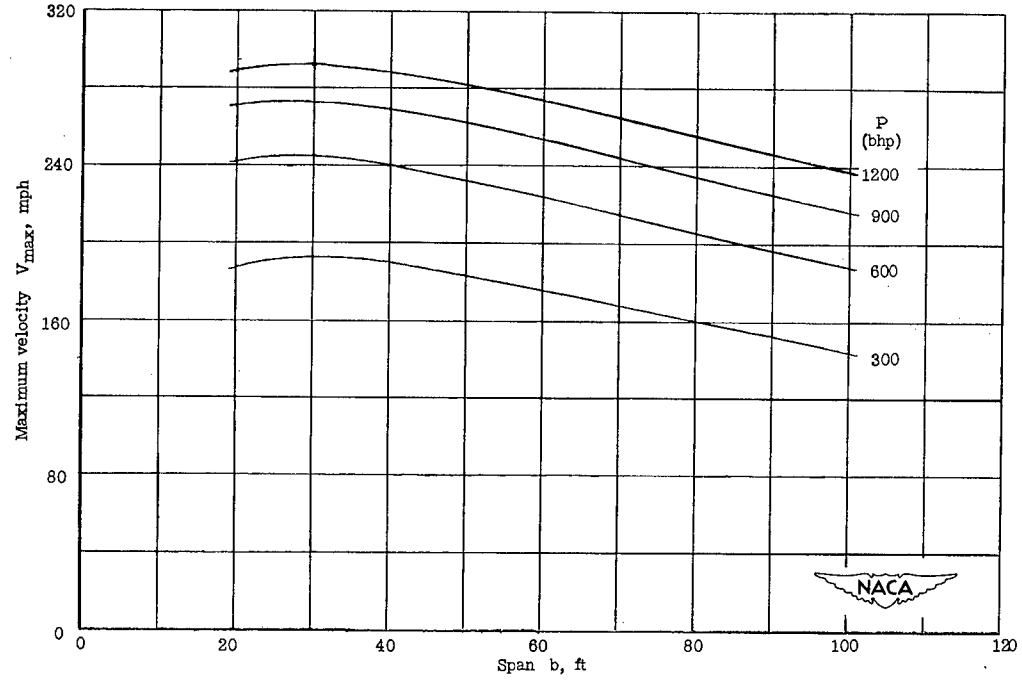

With boundary-layer control

(b) A = 10.

Figure 5.- Continued.

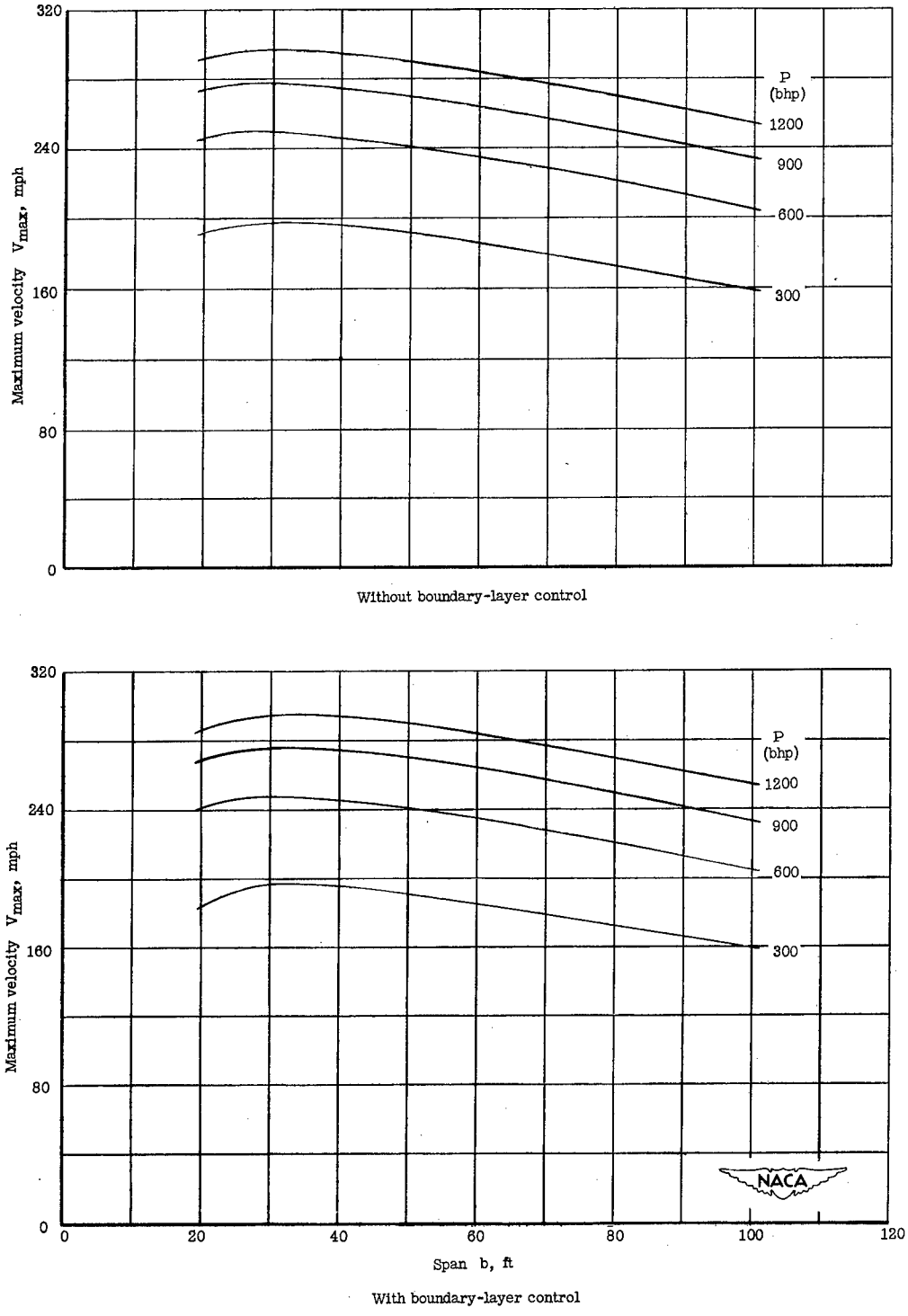

(c) A = 15.

Figure 5.- Concluded.

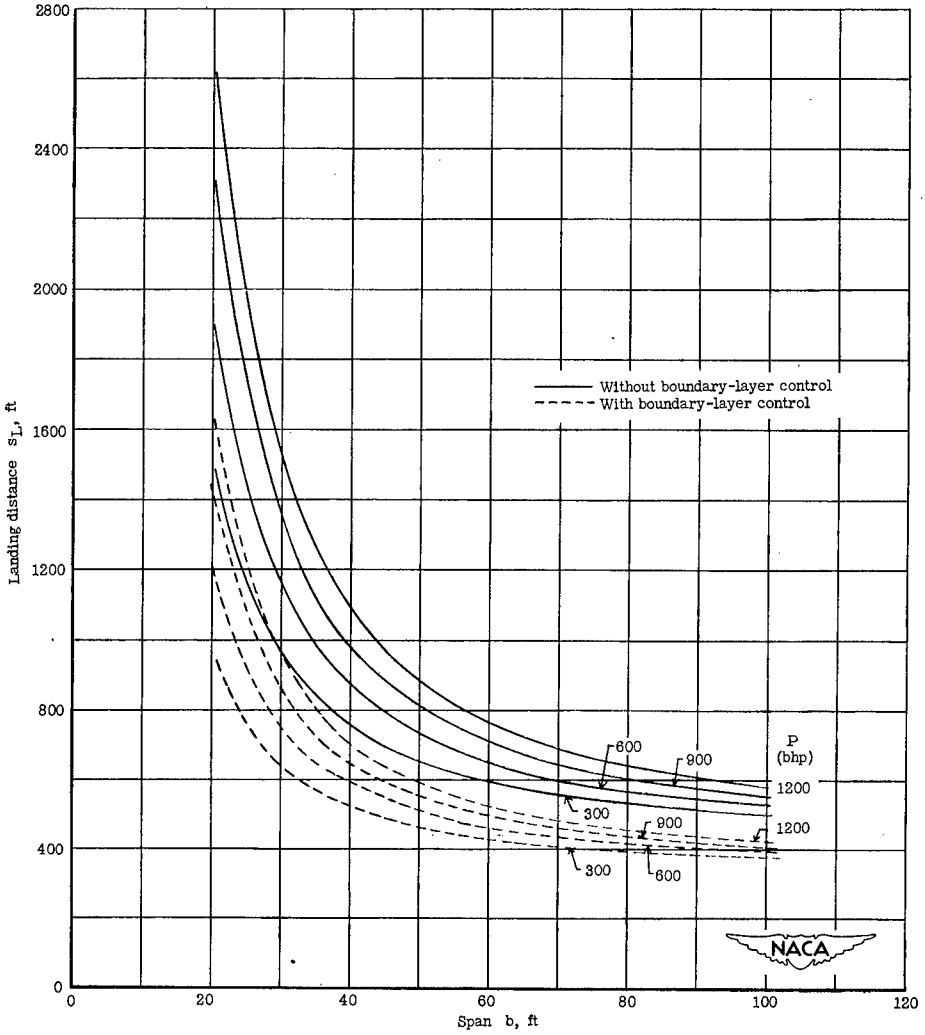

(a) A = 5.

Figure 6.- Landing distance of assumed airplane with and without boundary-layer control as a function of span for various powers.

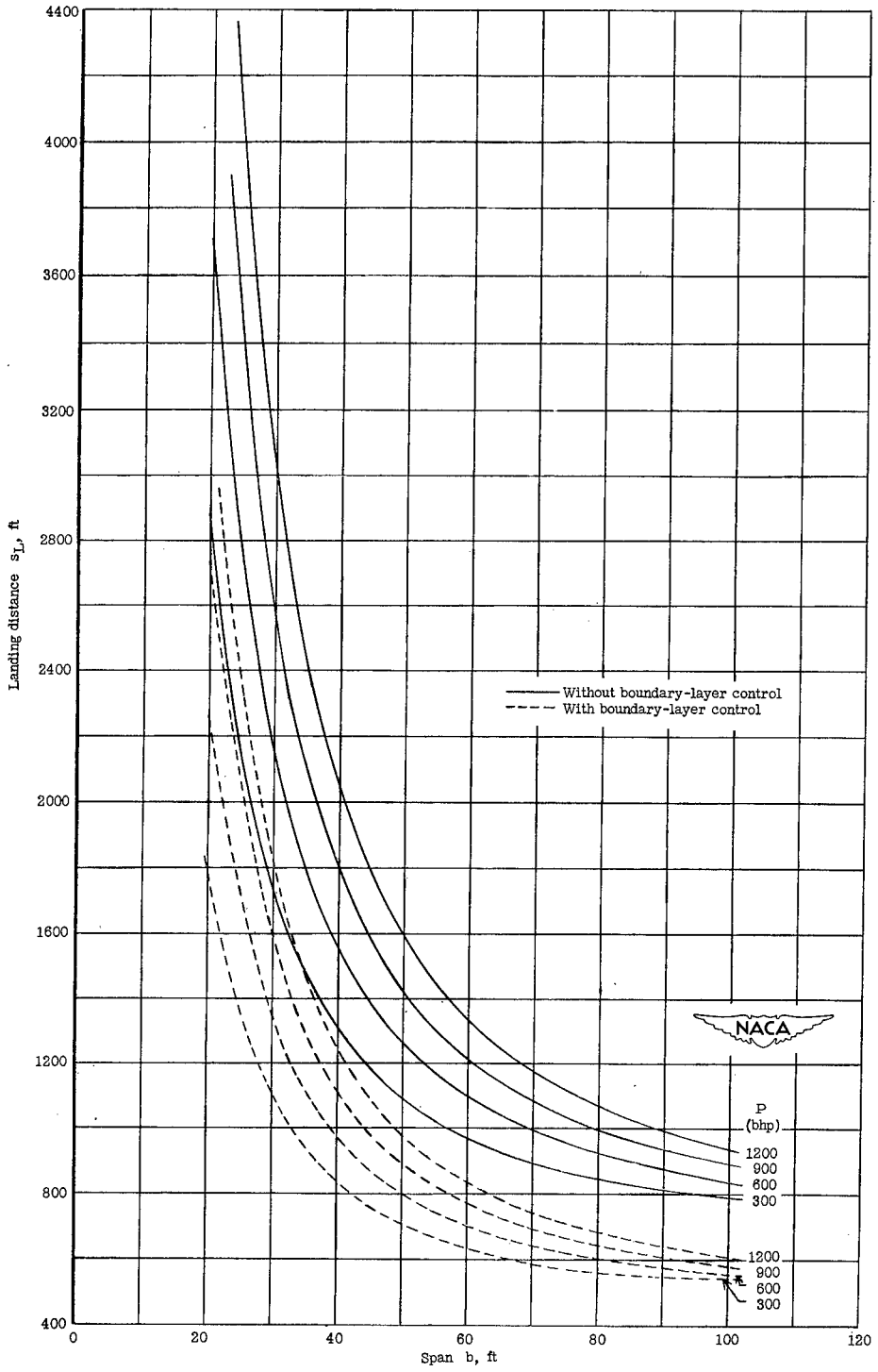

(b) A = 10.

Figure 6.- Continued.

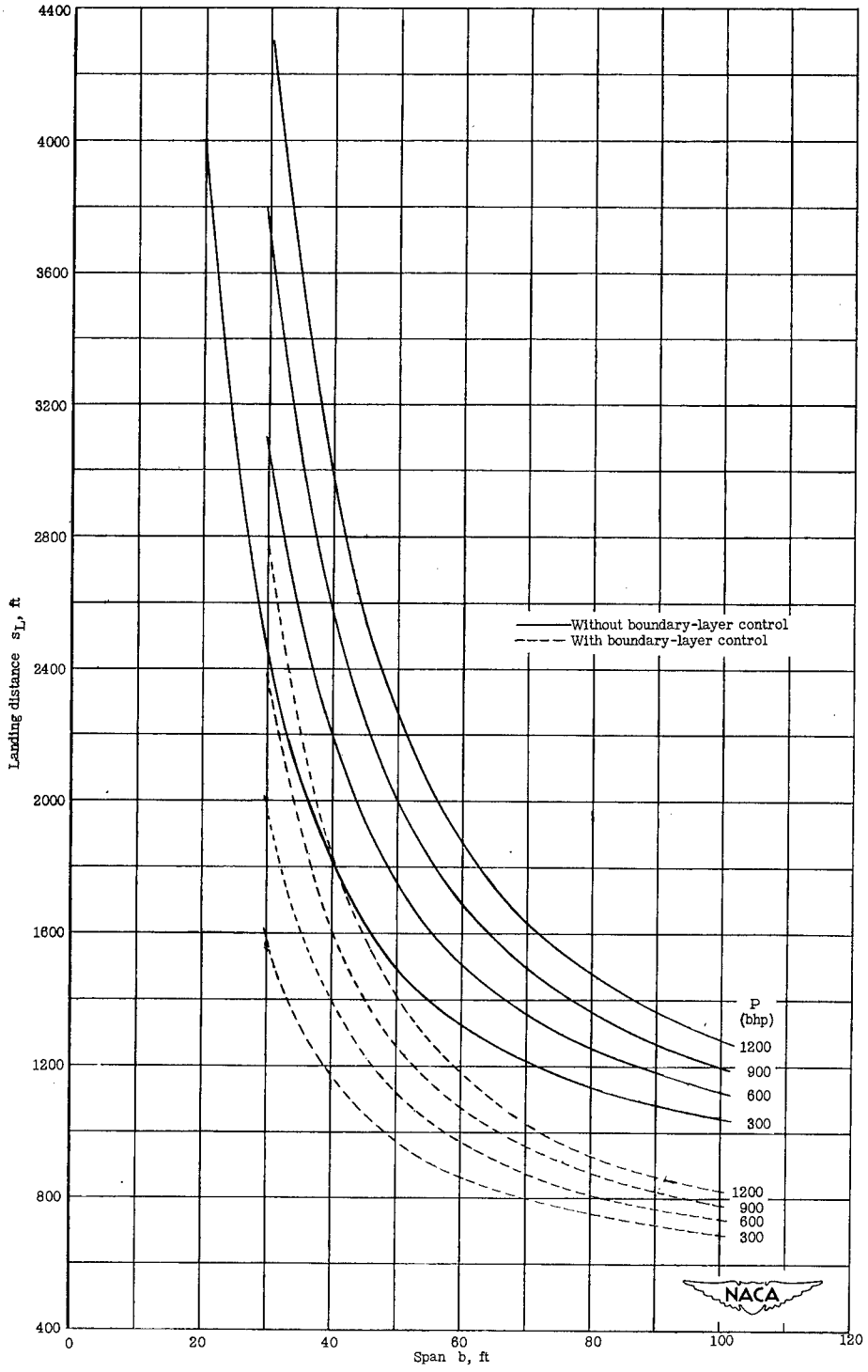

(c) A = 15.

Figure 6.- Concluded.

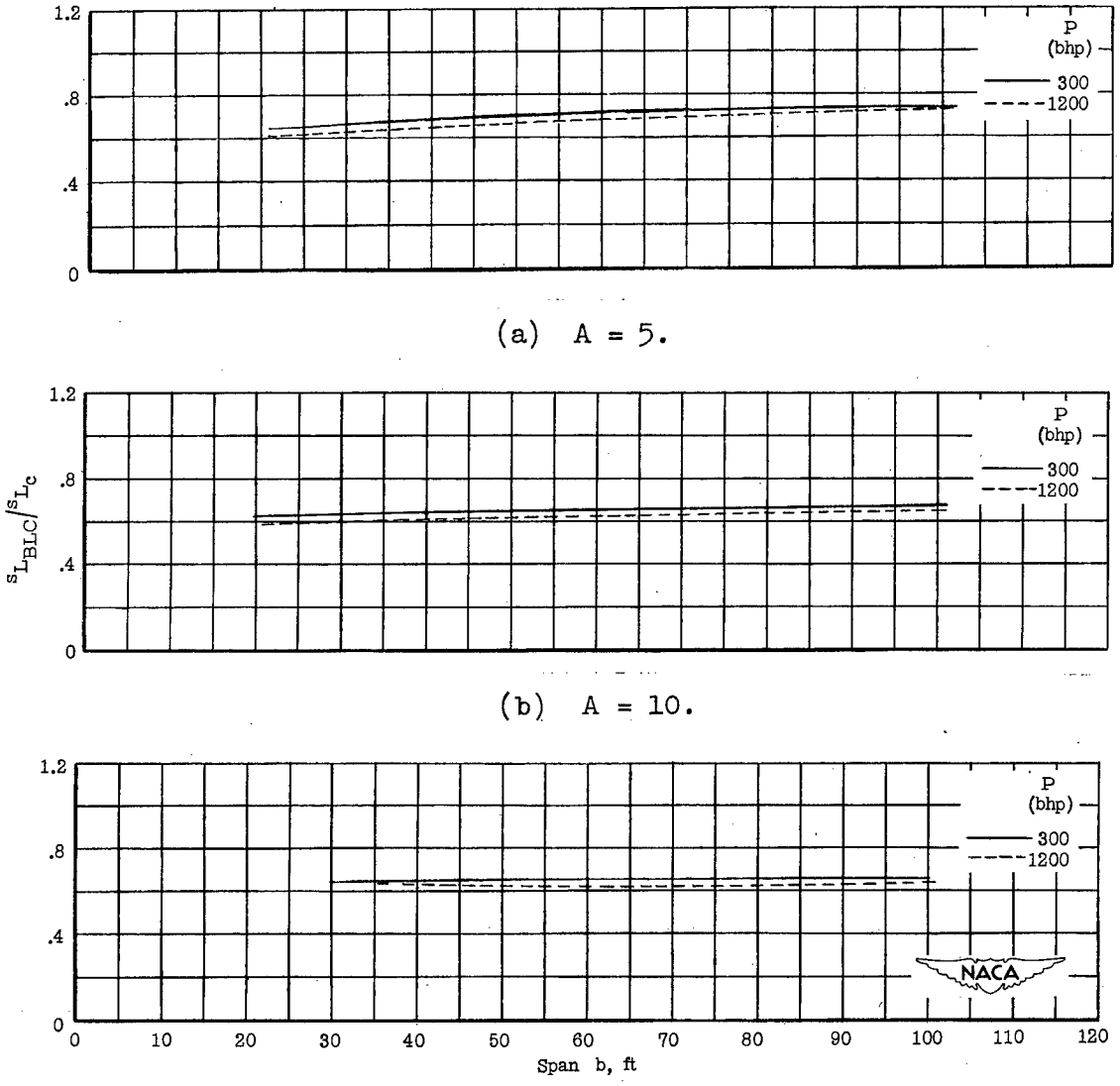

Figure 7.- Landing distance of airplane with boundary-layer control as a fraction of landing distance of same airplane without boundary-layer control.

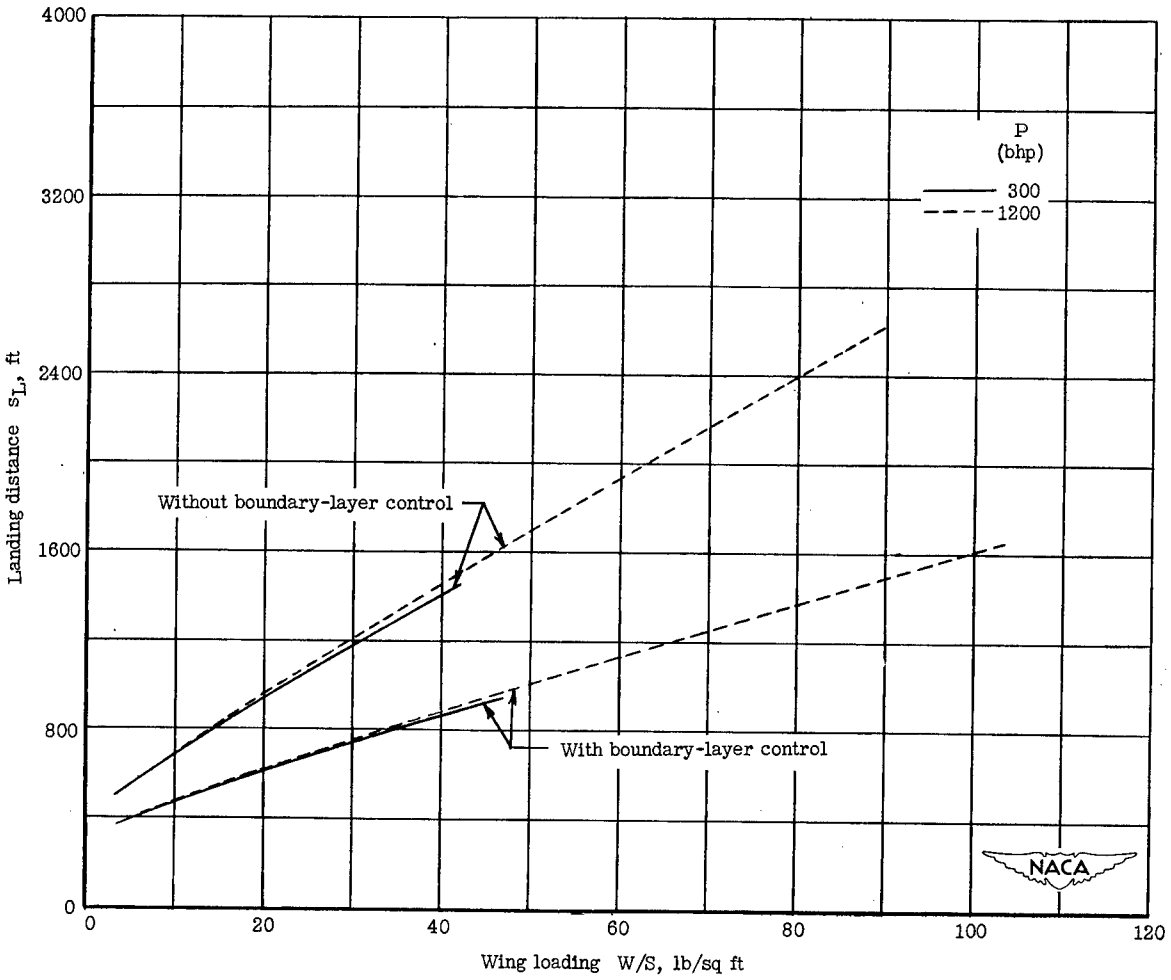

(a) A = 5.

Figure 8.- Landing distance of assumed airplane with and without boundary-layer control as a function of wing loading.

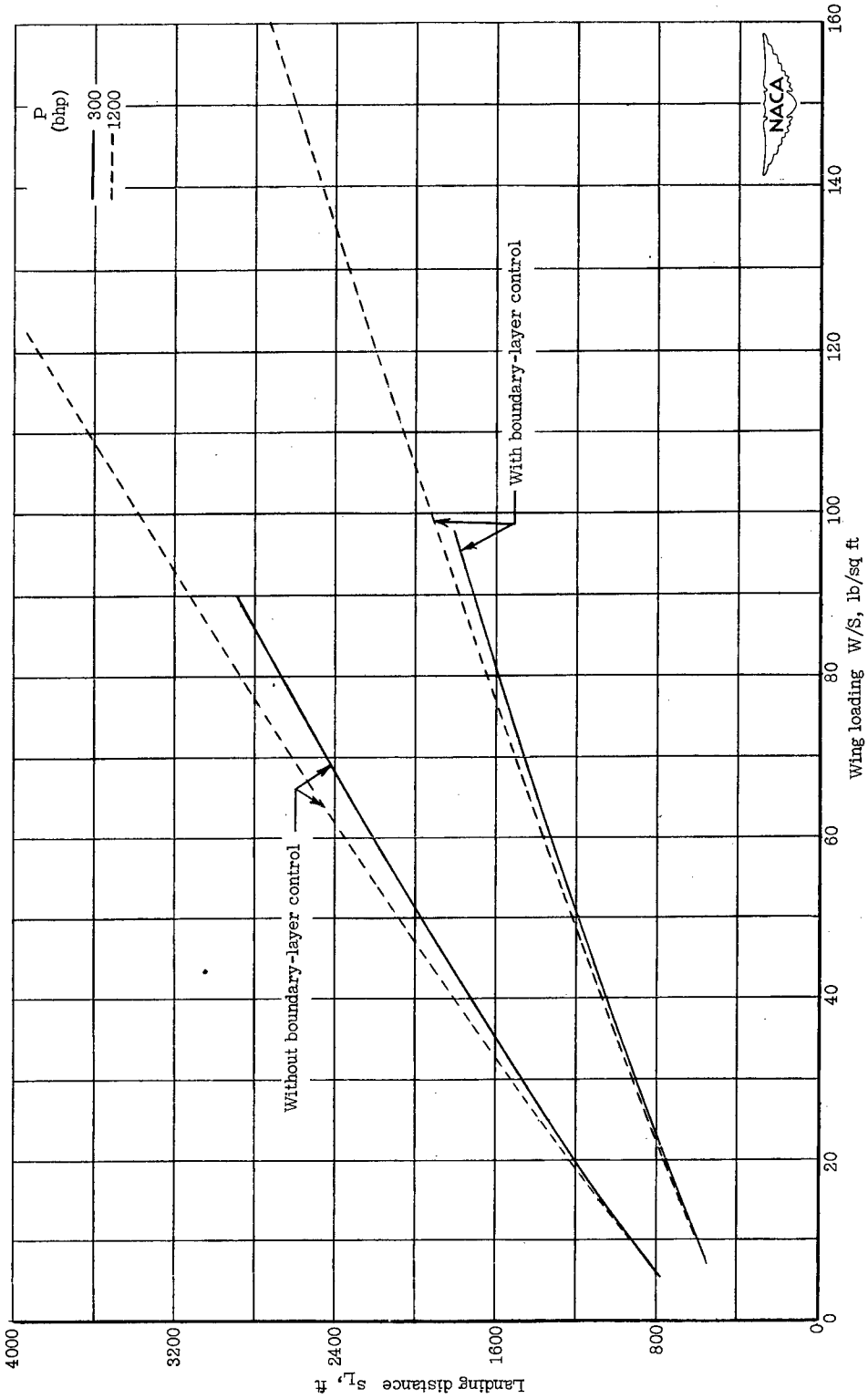

(b) A = 10.

Figure 8.- Continued.

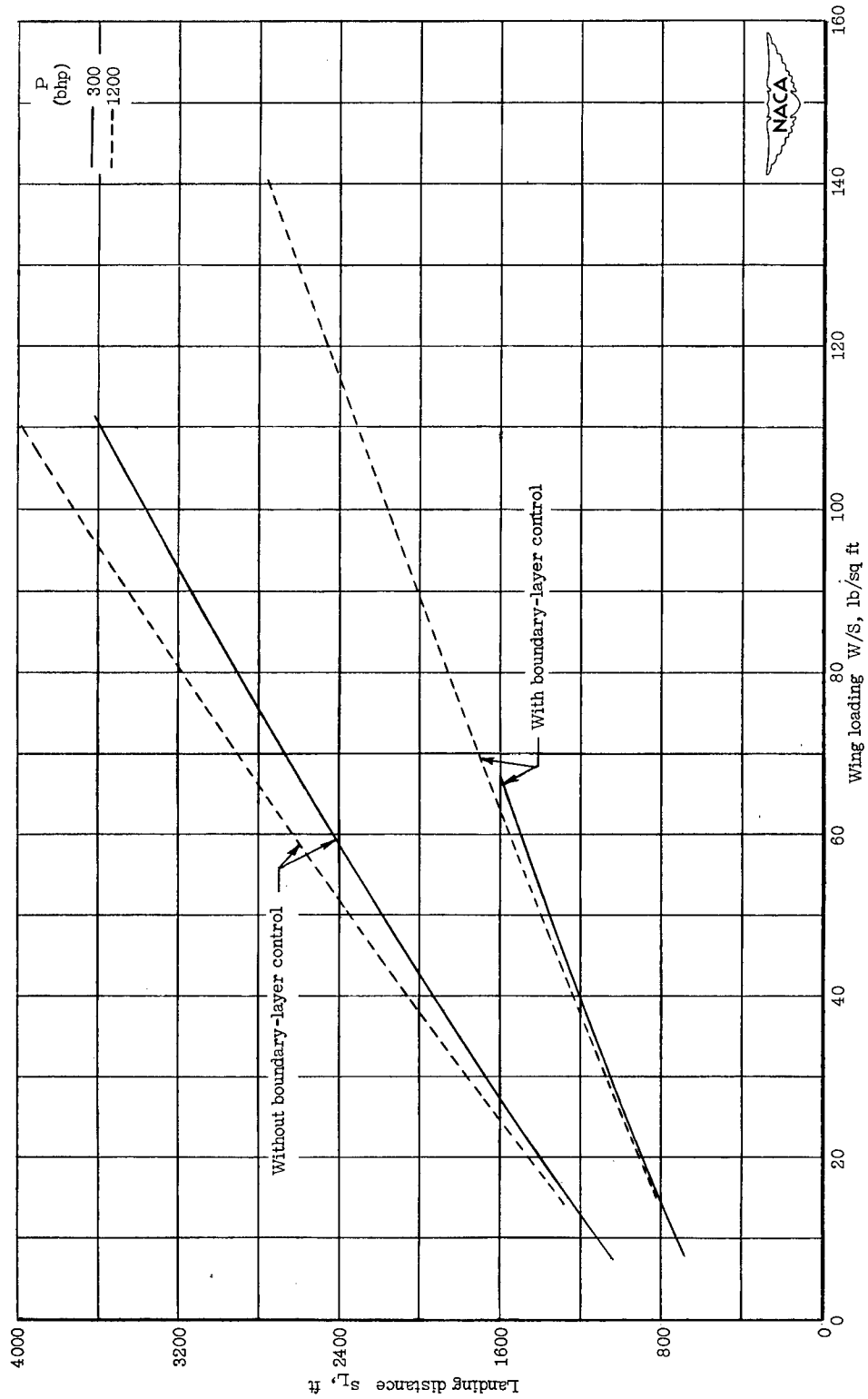

(c) A = 15.

Figure 8.- Concluded.

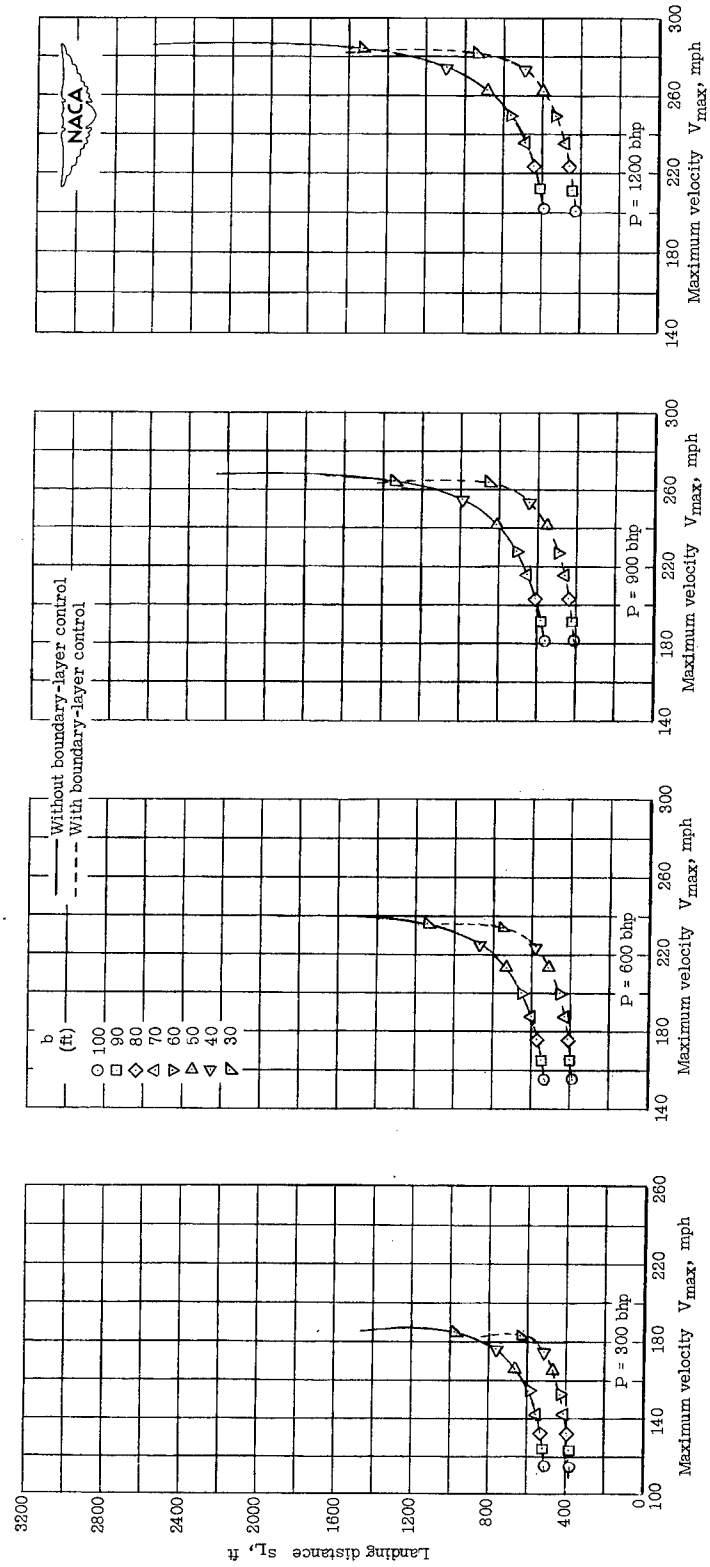

(a) A = 5.

Figure 9.- Landing distance of assumed airplane with and without boundary-layer control as a function of velocity for various powers.

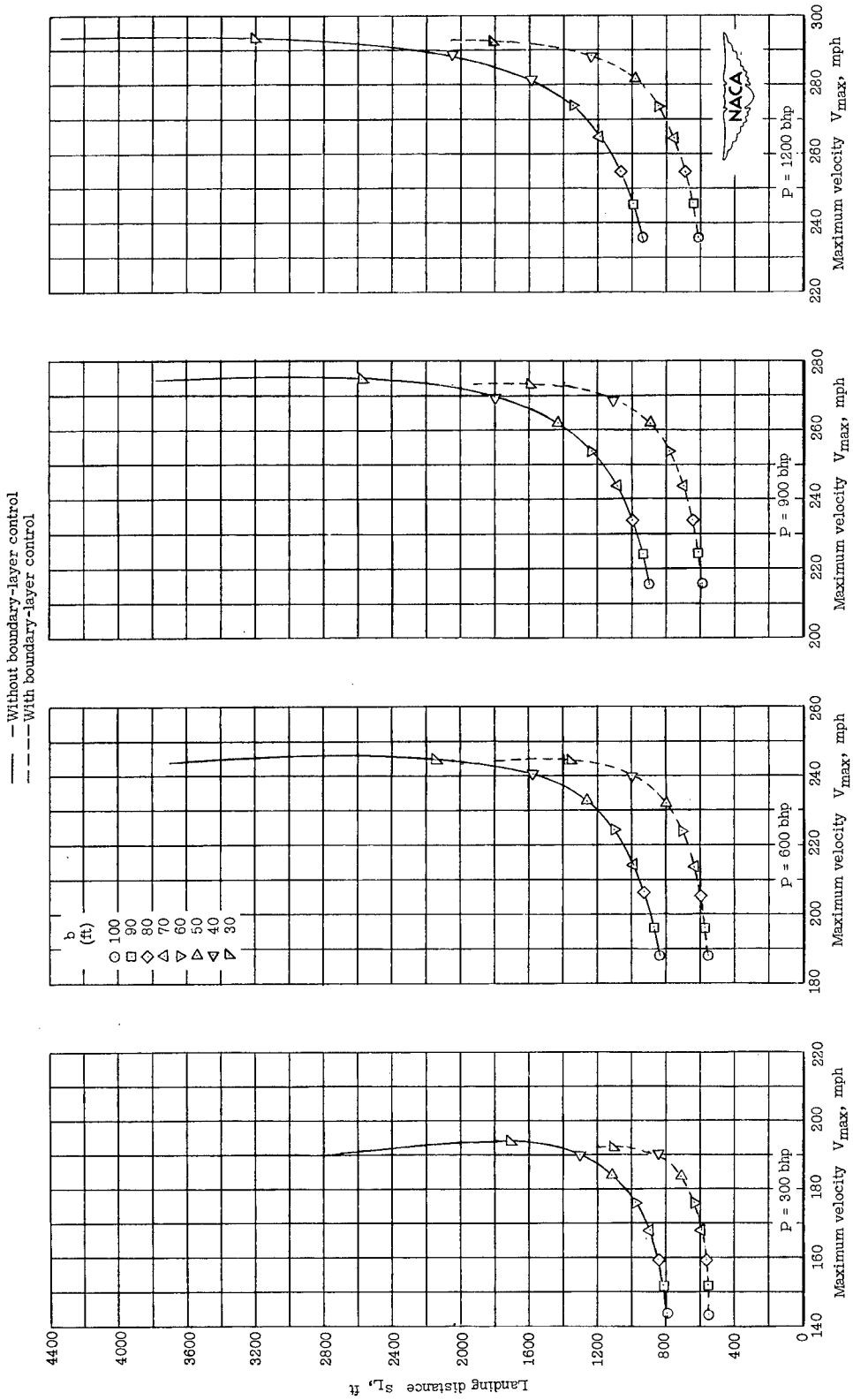

(b) A = 10.

Figure 9.- Continued.

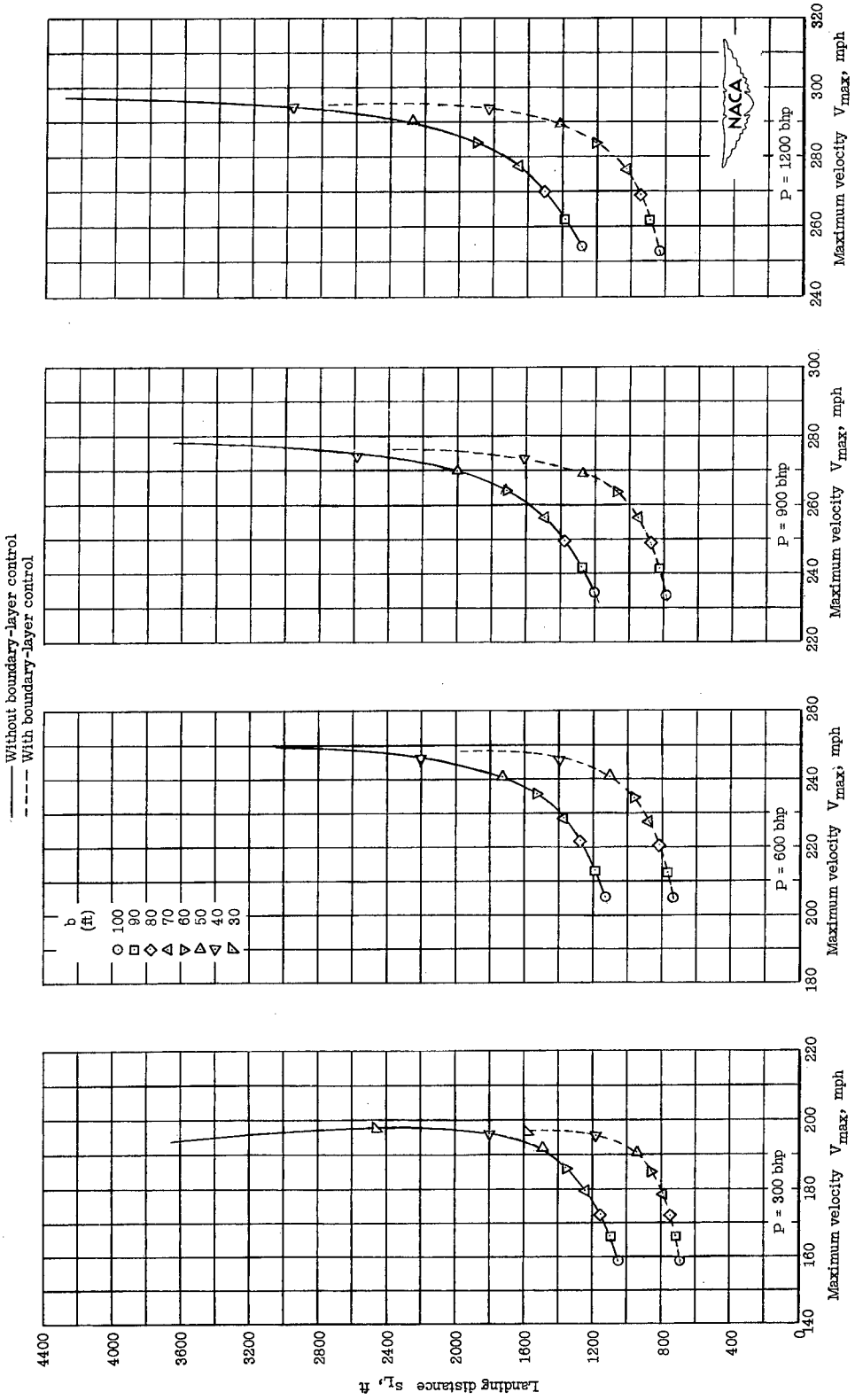

(c) A = 15.

Figure 9.- Concluded.

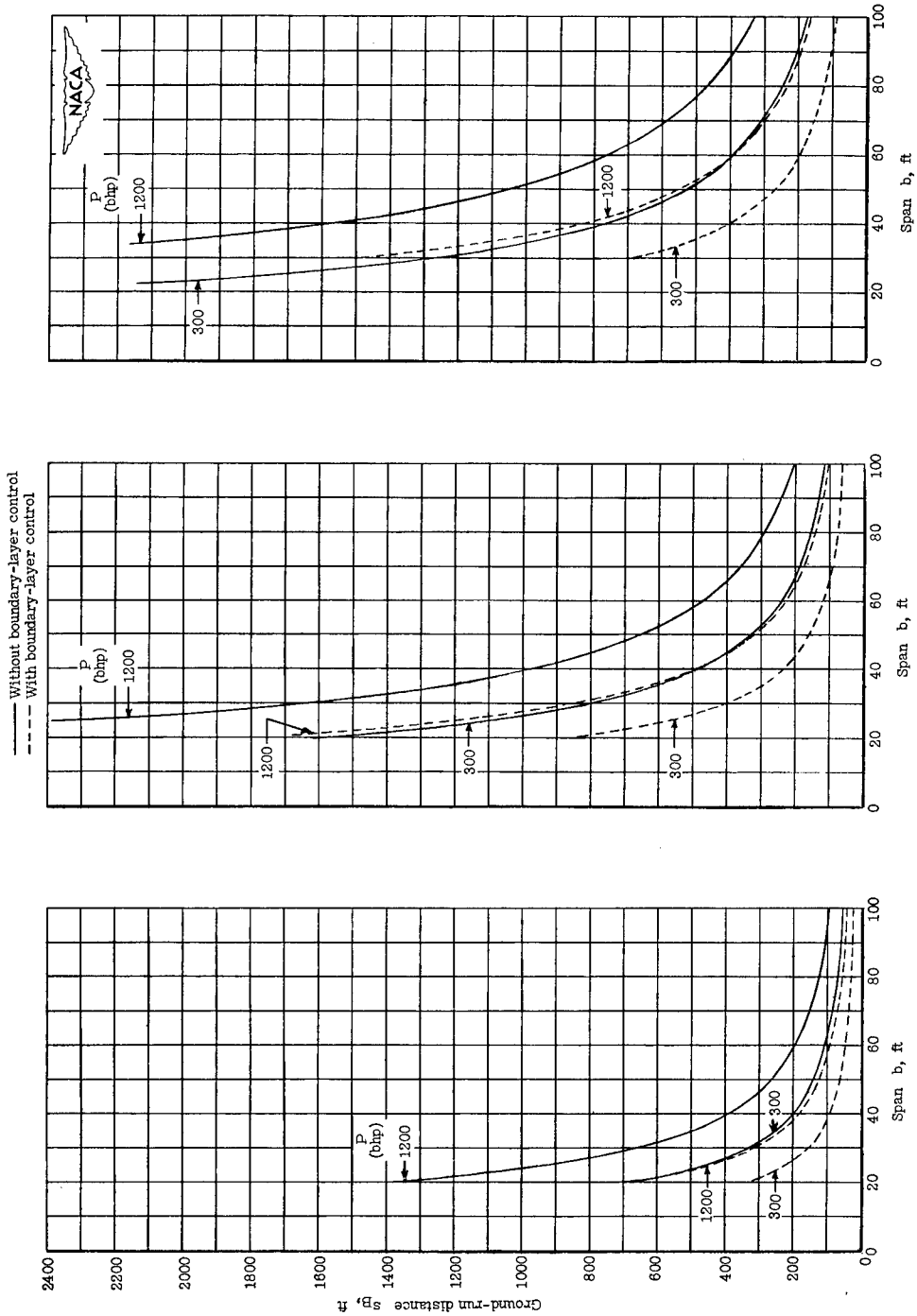

(a) A = 5. (b) A = 10. (c) A = 15.

Figure 10.- Ground-run distance of assumed airplane with and without boundary-layer control as a function of span.

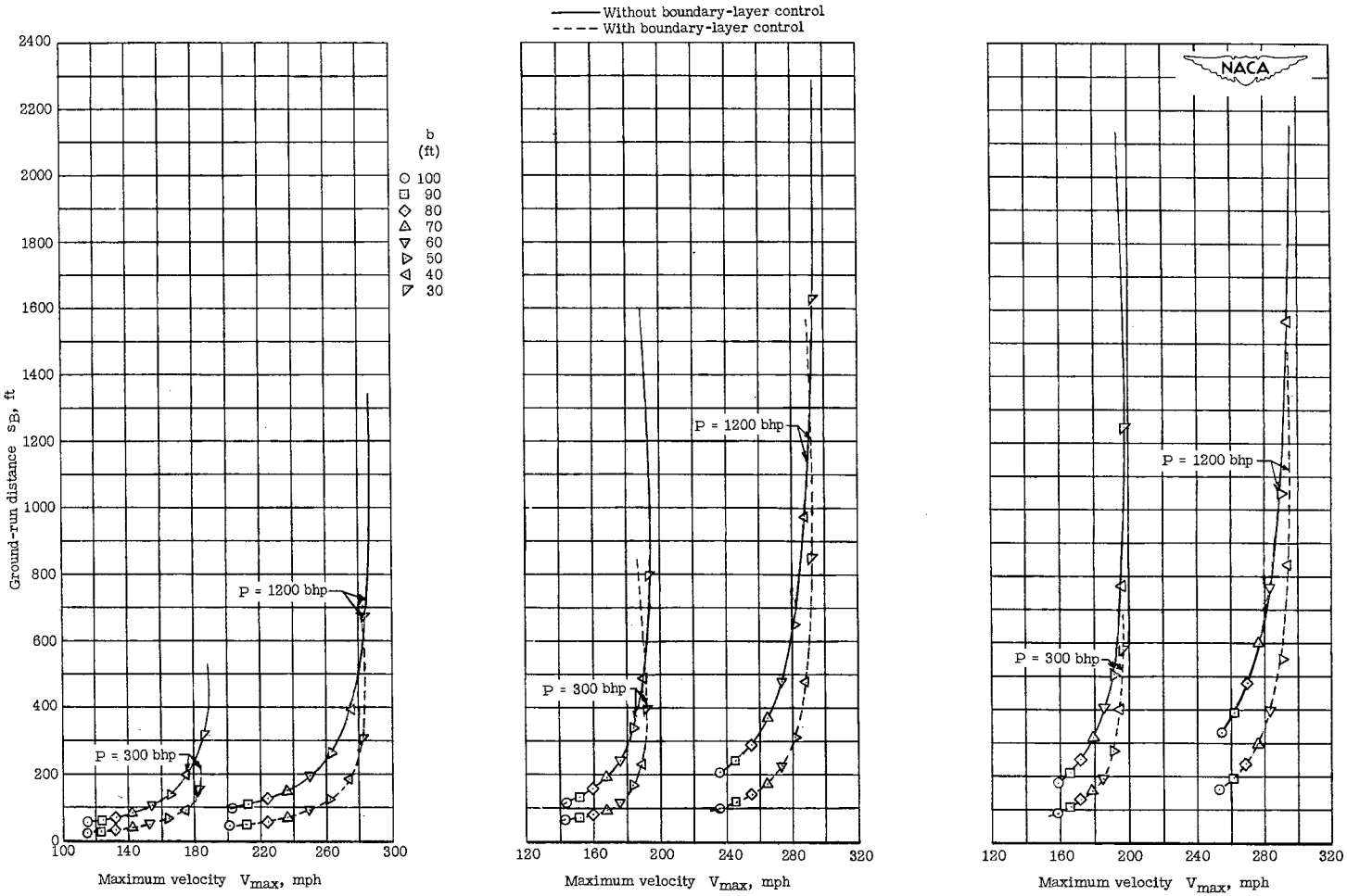

(a) A = 5. (b) A = 10. (c) A = 15.

Figure 11.- Ground-run distance of assumed airplane with and without boundary-layer control as a function of maximum velocity.

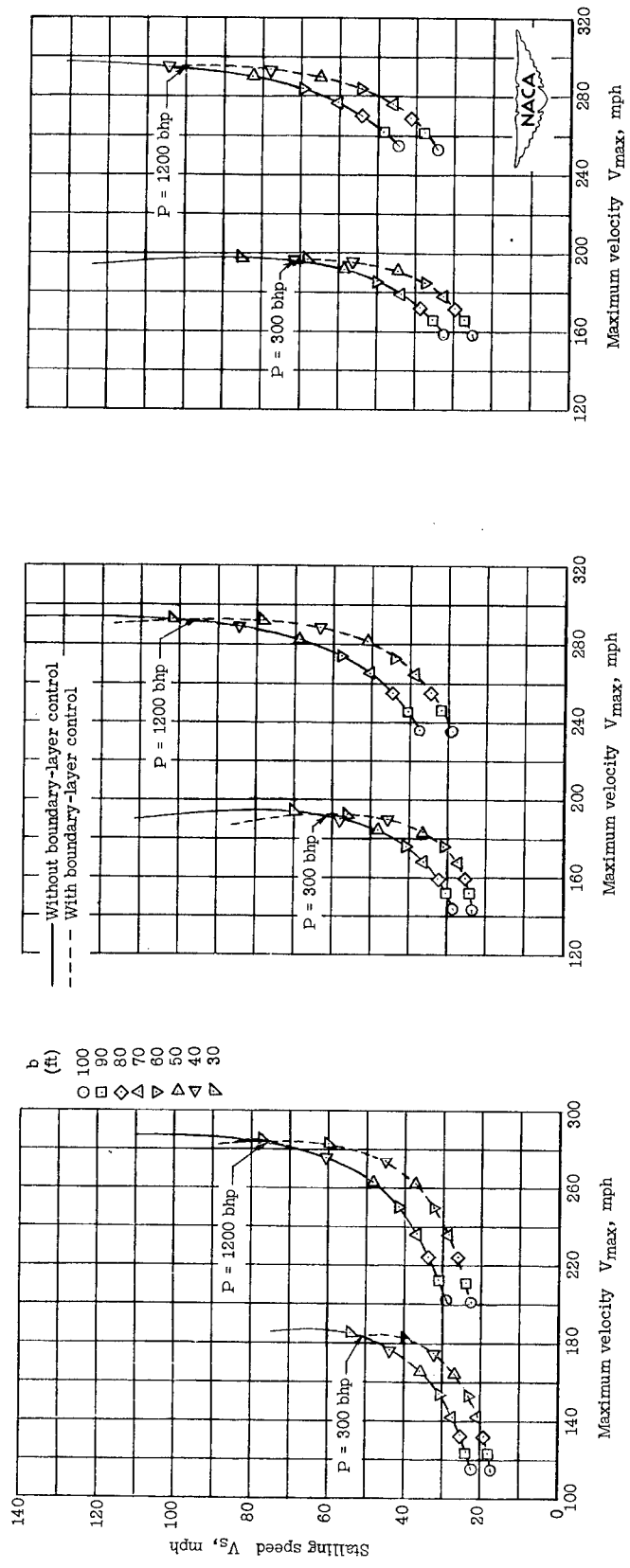

(a) A = 5. (b) A = 10. (c) A = 15.

Figure 12.- Stalling speed of assumed airplane with and without boundary-layer control as a function of maximum velocity.

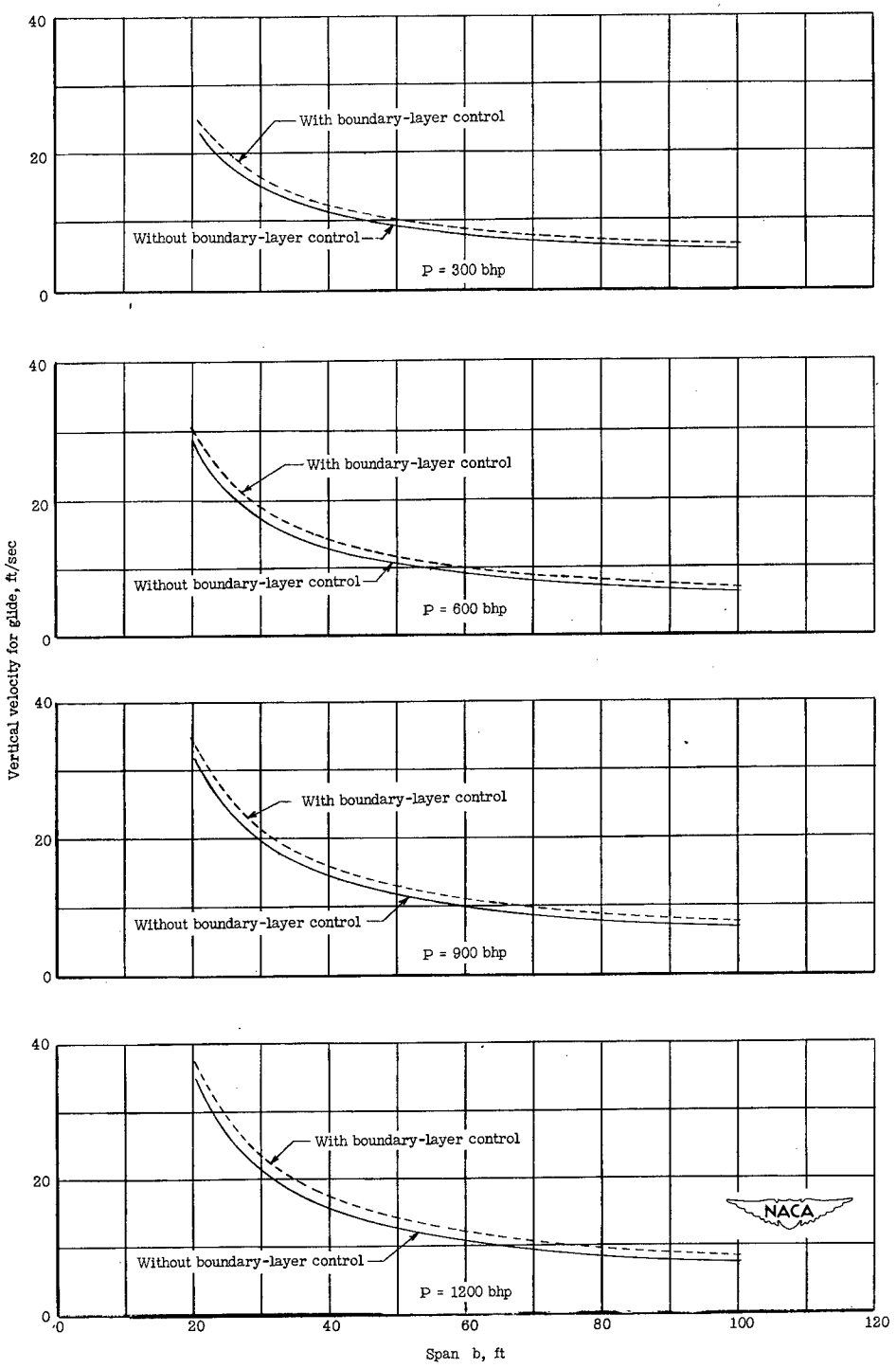

(a) A = 5.

Figure 13.- Vertical velocity as a function of span for assumed airplane with and without boundary-layer control.

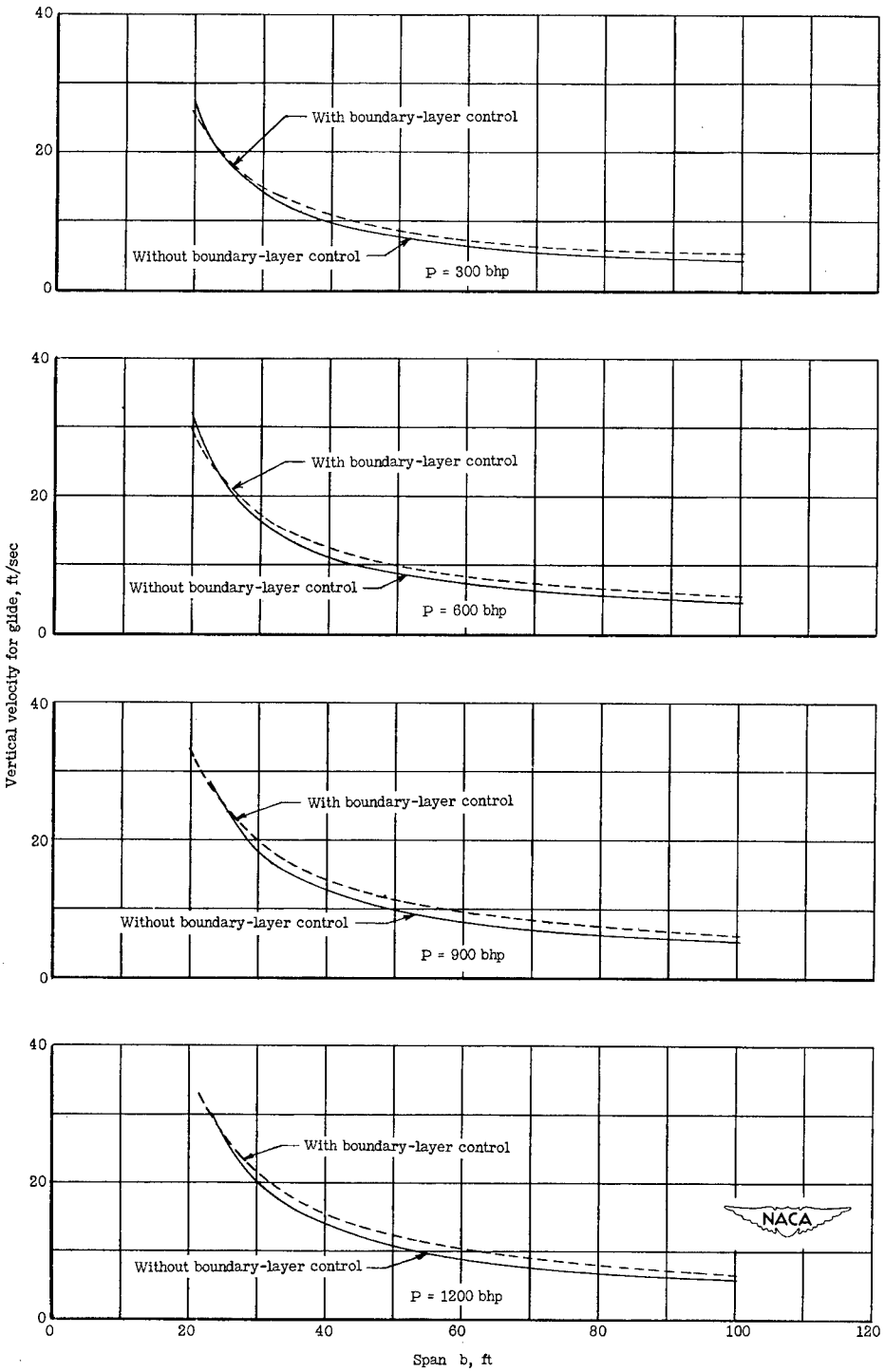

(b) A = 10.

Figure 13.- Continued.

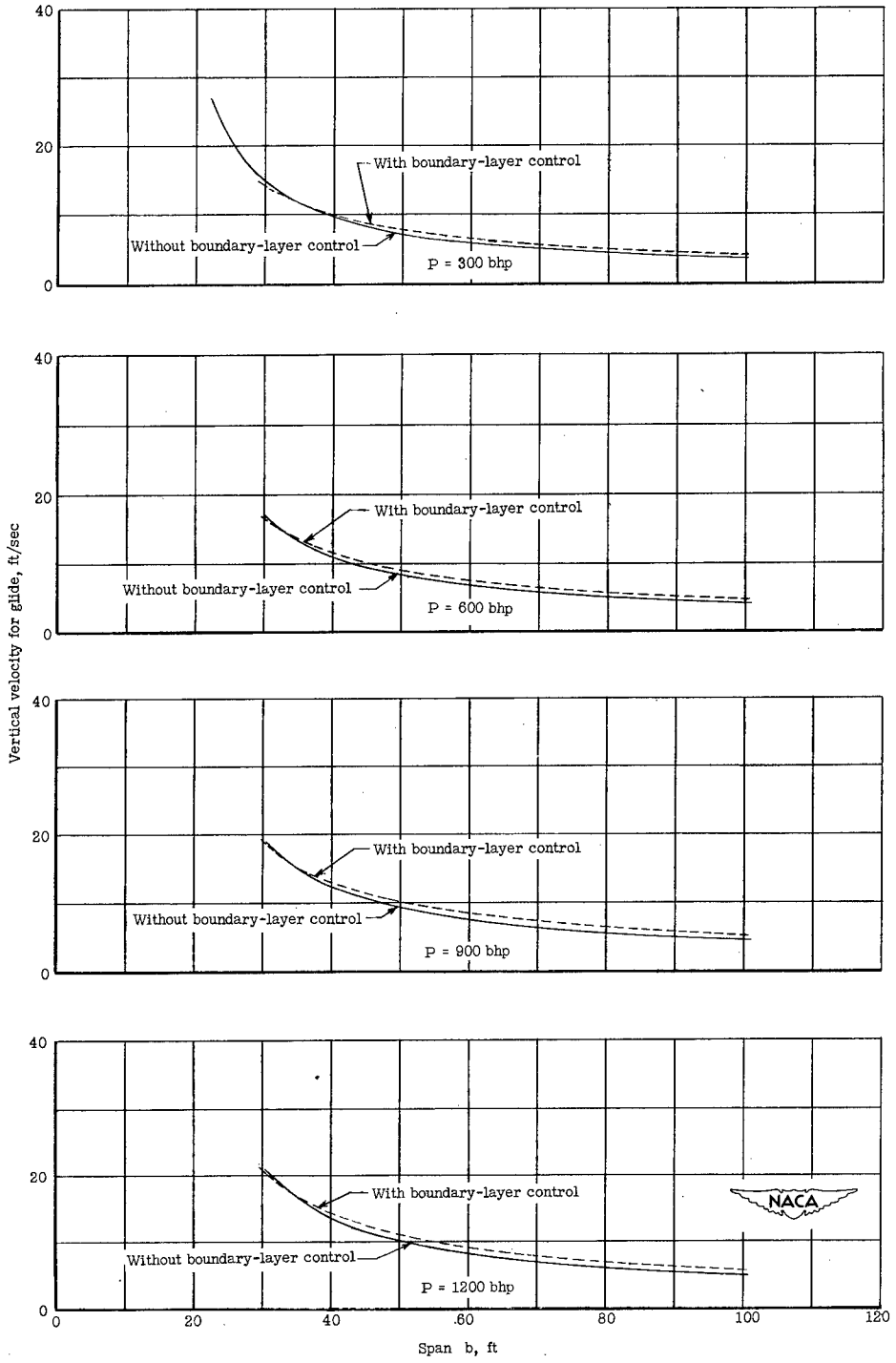

(c) A = 15.

Figure 13.- Concluded.

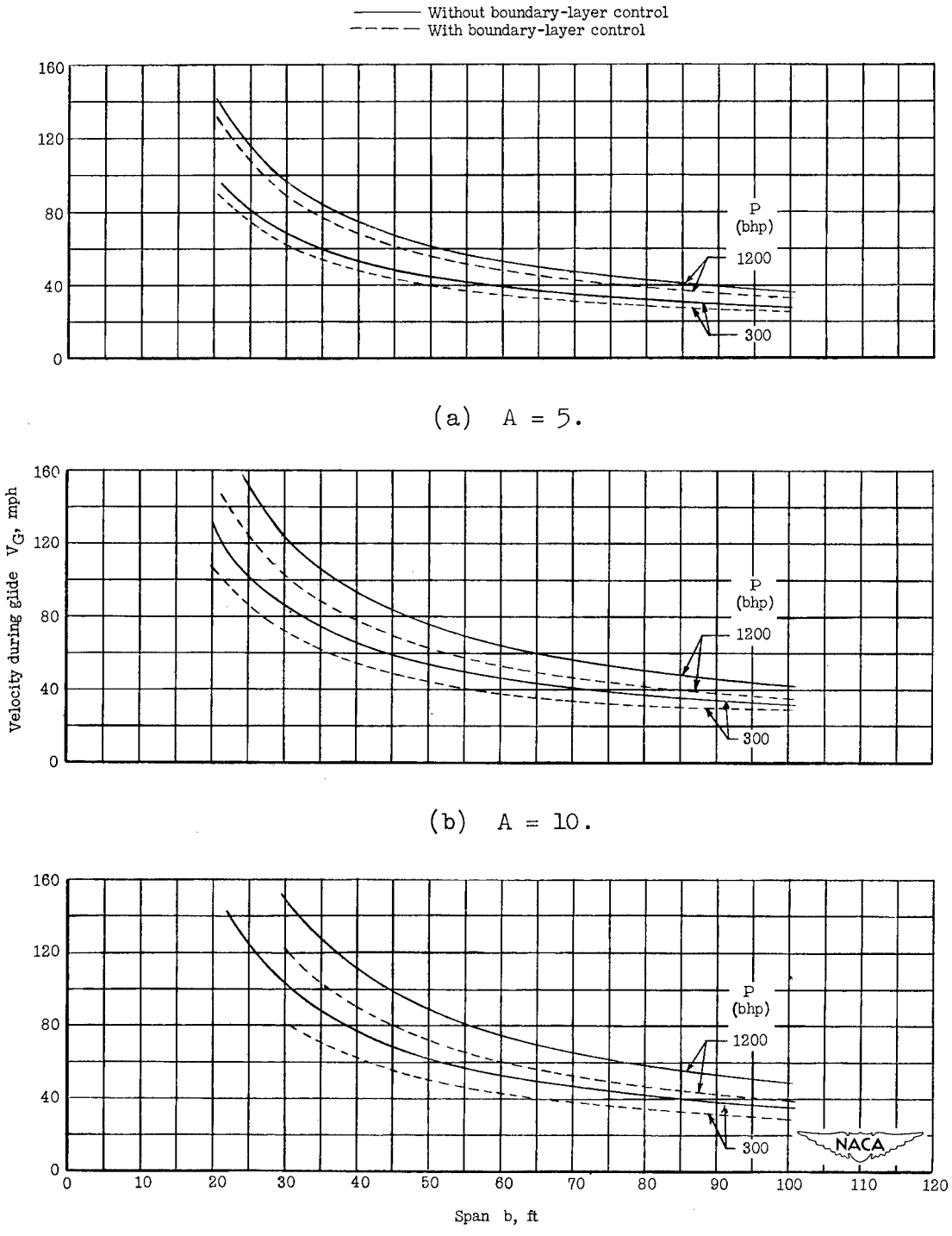

(a) A = 5.

(b) A = 10.

(c) A = 15.

Figure 14.- Velocity during glide for assumed airplane with and without boundary-layer control as a function of span.